General Disclaimer

One or more of the Following Statements may affect this Document

- This document has been reproduced from the best copy furnished by the organizational source. It is being released in the interest of making available as much information as possible.

- This document may contain data, which exceeds the sheet parameters. It was furnished in this condition by the organizational source and is the best copy available.

- This document may contain tone-on-tone or color graphs, charts and/or pictures, which have been reproduced in black and white.

- This document is paginated as submitted by the original source.

- Portions of this document are not fully legible due to the historical nature of some of the material. However, it is the best reproduction available from the original submission.

NASA CONTRACTOR REPORT 166519

(NASA-CR-166519) VTOL SHIPBOARD LETDOWN GUIDANCE SYSTEM ANALYSIS (Analytical Mechanics Associates, Inc.) 60 p
HC A04/MF A01 CSCL 01C G3/08

N84-25716
Unclas
13561

VTOL Shipboard Letdown Guidance System Analysis

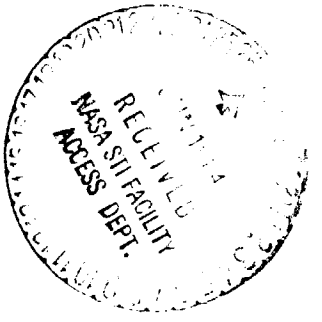

A.V. Phatak
M.S. Karmali

CONTRACT NAS2- 10288
May 1983

NASA

NASA CONTRACTOR REPORT 166519

VTOL Shipboard Letdown Guidance System Analysis

Anil V. Phatak
Mehebub S. Karmali
Analytical Mechanics Associates, Inc.
2483 Old Middlefield Way
Mountain View, CA 94035

Prepared for
Ames Research Center
Under NASA Contract NAS2-10288

National Aeronautics and
Space Administration

Ames Research Center
Moffett Field, California 94035

PREFACE

This effort was performed under Contract No. NAS2-10288 from the NASA Ames Research Center. Mr. Clyde H. Paulk, Jr. was the Technical Monitor for this project.

The project manager at AMA, Inc. was Dr. Anil V. Phatak. The project engineer was Mr. Mehebub S. Karmali. Programming support was provided by Ms. Susan Dorsky. Technical discussions with Dr. Stanley F. Schmidt and Dr. John A. Sorensen of AMA, Inc. are acknowledged.

ABSTRACT

This report examines alternative letdown guidance strategies for landing of a VTOL aircraft onboard a small aviation ship under adverse environmental conditions. Off-line computer simulation of shipboard landing task is utilized for assessing the relative merits of the proposed guidance schemes. A sum of seventy sinusoids representation is used to model the ship motion time histories. The touchdown performance of a nominal constant-rate-of-descent (CROD) letdown strategy serves as a benchmark for ranking the performance of the alternative letdown schemes.

Analysis of ship motion time histories indicates the existence of an alternating sequence of quiescent and rough motions called "lulls" and "swells". A real time algorithm for lull/swell classification based upon ship motion pattern features is developed. The classification algorithm is used to command a go/no go signal to indicate the initiation and termination of an acceptable landing window. Simulation results show that such a go/no go pattern based letdown guidance strategy provides an order of magnitude improvement in touchdown performance over that obtained with the nominal CROD letdown scheme.

TABLE OF CONTENTS

LIST OF FIGURES

1. INTRODUCTION

An important problem in naval aviation is the landing of a VTOL aircraft onboard a small ship under adverse weather conditions. Typically, the shipboard landing problem is divided into two distinct phases: (1) a decelerating approach to a stationkeeping (hover) point near the stern, followed by (2) a letdown or descent from hover to a landing on the ship's deck. A sketch illustrating the relative geometry of the shipboard landing scenario is shown in Figure 1. Both the aircraft and the ship landing pad motions are defined with respect to a local level reference frame (X_D, Y_D, Z_D) centered at the average position of the bullseye with the three axes along the ship's stern, starboard and up directions, respectively. The stationkeeping point (x_h, y_h, z_h) represents the position of the aircraft upon termination of the approach phase and prior to the initiation of the letdown maneuver.

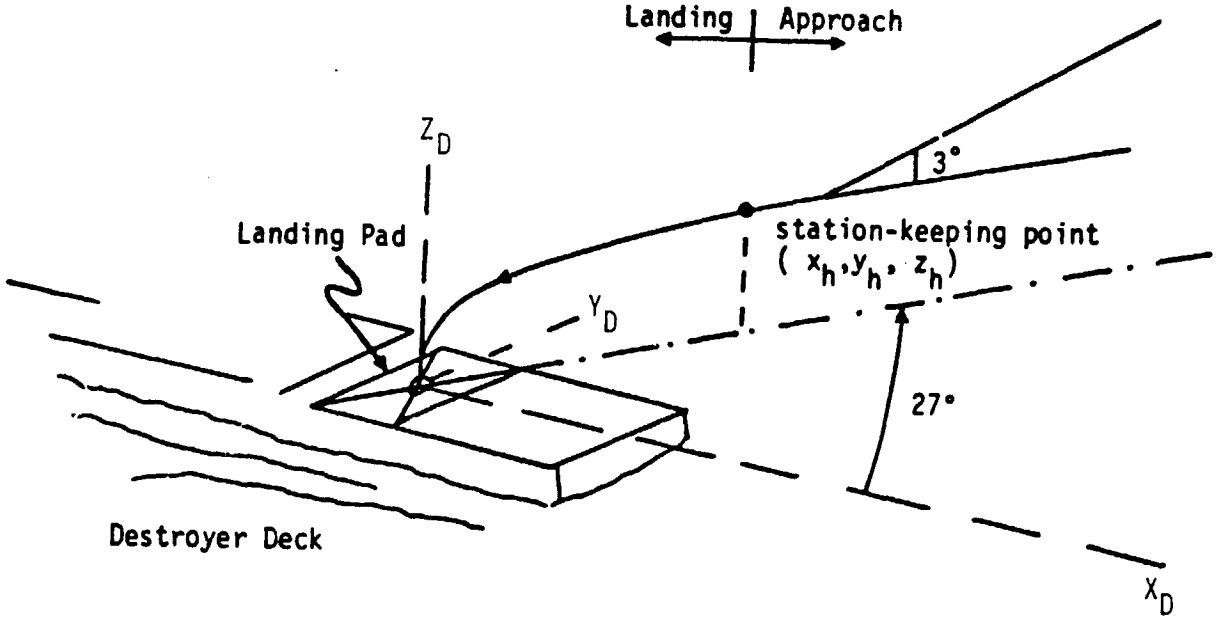

Figure 1. Shipboard Landing Scenario

The primary task during letdown is to bring the aircraft from the hover point to a touchdown onboard the ship's landing pad (approximately 40 x 40 ft^2) in a safe and efficient manner. As a minimum, the aircraft should be able to land on the deck without damaging its landing gear or skidding off the deck. This requirement translates into specific limits upon the acceptable relative translational and angular positions and velocities of the aircraft with respect to the landing pad at touchdown. Additional constraints on the ship landing pad position and orientation at touchdown ma be necessary from an operational viewpoint. The nature of these constraints would depend upon a number of factors, including: (a) the aircraft-control system capabilities/limitations, (b) landing gear specifications and post-touchdown aircraft recovery procedures e.g., existence of clasping or clamping mechanisms onboard the ship, (c) pilot-centered human factors guidelines, and (d) environmental and safety considerations.

Thus two questions are posed:

1. What is an acceptable landing?

2. What percentage of the touchdowns would be acceptable if only a constant rate-of-descent letdown guidance is commanded to the aircraft?

The first question may be answered by introducing the concept of an acceptable landing envelope defined as a region in which the relative translational and rotational state of the aircraft with respect to the pad at touchdown is within some prescribed bounds. Given such a definition of an acceptable landing, an answer to the second question should indicate whether a constant rate-of-descent letdown is adequate. Otherwise, a landing guidance system must be developed to assure bringing the aircraft to an acceptable touchdown under varying environmental conditions.

The purpose of this research effort has been to identify, define and analyze factors relevant to the successful landing of VTOL aircraft onboard a small aviation ship under adverse environmental conditions. The ultimate

objective had been the investigation of alternate landing guidance concepts for improving touchdown performance over that achievable with a constant rate-of-descent letdown. Off-line computer simulation of the shipboard landing task was utilized as the principal tool for investigating the relative merits of the proposed alternative landing guidance concepts.

This effort represents one aspect of the overall problem of shipboard VTOL operations. The ideas and concepts developed in this study draw upon the work of previous studies, to some extent. Therefore, key sources are referenced throughout this document.

This report consists of five sections. Section 2 describes the various elements that must be integrated into a simulation of the VTOL shipboard landing task. Particular emphasis is given to the simulation of six degree of freedom (DOF) ship/deck motion using a sum of sinusoids representation. The concept of an acceptable landing envelope is defined and the touchdown performance of a constant rate-of-descent letdown controller is analyzed. Following this, a discussion of alternative letdown guidance strategies is presented. Among the options, a go/no go letdown decision concept based upon the existence of a ship motion pattern of alternating quiescent periods called "lulls" and large motion inter-lull intervals called "swells" appears to be the most promising from a practical real-time implementation viewpoint.

Section 3 is devoted to the investigation of lull/swell patterns in ship/deck motion. An analytical definition of ship motion lulls is presented and utilized in the formulation of a real-time algorithm for lull/swell classification. Statistics of lull and swell durations and motions are analyzed as a function of the algorithmic parameters.

Section 4 discusses the improvements in touchdown performance obtained with a ship motion pattern based letdown guidance strategy.

Section 5 summarizes the conclusions derived from the study and outlines a cockpit simulator test program for verifying the project findings.

2. SHIPBOARD LANDING GUIDANCE

In order to develop an off-line computer simulation of the VTOL shipboard landing task, it is necessary to have suitable mathematical models for the individual elements that characterize the landing environment. Therefore, a realistic simulation must include models for (a) the ship/deck motion, (b) the airwake turbulence due to the ship's superstructure, (c) the aircraft dynamics including the characteristics of the associated flight control system, (d) the shipboard and airborne navigation system, and finally, (e) the landing guidance system. However, the principal objective of this study has been the analysis of VTOL landing guidance system requirements to ensure acceptable impact conditions at touchdown onboard a moving ship under rough sea conditions. The primary factor which makes shipboard landing so difficult is the existence of large and apparently unpredictable excursions in landing pad position (primarily heave) and orientation (mostly roll and pitch deviations) caused by the wave disturbances in a high sea state ($\geq$ 5) environment. Therefore, greatest emphasis was placed during this study on realistic ship motion simulation. Ship airwake turbulence and deck proximity effects are not considered. Furthermore, it is assumed that the airborne equipment has access to exact: (a) ship attitude, (b) aircraft attitude, and (c) aircraft and landing pad position coordinates in a local level reference frame centered at the average position of the ship's center of gravity or bullseye. The aircraft control system is assumed to provide first or second order step response characteristics in the angular and translational degrees of freedom. Details of the system bandwidth and time constant parameters are discussed in section 2.4 where alternate landing guidance and controller concepts are considered.

2.1. Ship Motion Simulation

The NAVAIRENGCEN Ship Motion Computer Program [1] was used in this study to generate ship motion time history data. The program is based

on a technique for modeling ship motions that was introduced by St. Denis and Pierson in their classic paper "on the Motions of Ships in Confused Seas" [2]. The approach consists of representing the ship motion in each of the six degrees of freedom (roll, pitch, yaw, surge, sway, heave) at the ship's center of gravity (CG) by a sum of sinusoids. Selection of the number of sinusoids and their amplitudes, frequencies and relative phase angles is based upon having a dynamical ship model, as shown in Figure 2, for computing the ship motion response to wave disturbance inputs. Ship motion response $\eta(t)$ is related to the wave input $\zeta(t)$ through the ship transfer function (also referred to as the regular wave transfer function in Ref. 1) $H_\eta(j\omega)$.

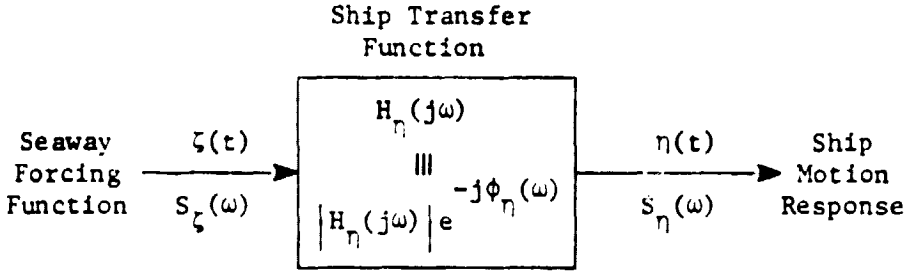

Figure 2. Ship Motion Response Computation

The seaway or wave disturbance $\zeta(t)$ is defined to be a stationary ergodic random process with power spectrum $S_\zeta(\omega)$, where ω is the frequency (rad/s) of the wave inputs. Note that the definition of spectral density in wave theory is slightly different than the standard form used in linear systems theory. Thus, spectral density in wave theory is defined as:

$$\begin{aligned} S_x(\omega) &\triangleq \frac{1}{\pi}\int_{-\infty}^{\infty} R_x(\tau)\, e^{-j\omega\tau}\, d\tau \quad : \ \omega \geq 0 \\ &\triangleq 0 \quad : \ \omega \leq 0 \end{aligned} \tag{1}$$

Similarly, autocorrelation is defined as

$$R_x(\tau) \triangleq \int_0^{\infty} \mathrm{Re}\left[S_x(\omega) e^{j\omega\tau}\right] d\omega \tag{2}$$

Thus, mean square value of x(t) is

$$\overline{x^2} = \int_0^\infty S_x(\omega)\, d\omega \,. \tag{3}$$

For the purpose of this study, the Bretschneider spectrum [1] is used to represent the wave spectra. Thus,

$$S_\zeta(\omega) \triangleq \frac{A}{\omega^5} \exp\left(\frac{-B}{\omega^4}\right) \tag{4}$$

where $A = \frac{483.5}{T_0^4} \cdot \zeta_{1/3}^2$

$B = \frac{1944.5}{T_0^4}$

$\zeta_{1/3}$ = significant wave height (average double amplitude of the one third highest waves)

and T_0 = modal period.

Figure 3 shows the normalized Bretschneider spectrum for various values of T_0. Note that the modal period T_0 can be used to adjust the peak magnitude frequency ω_{max} according to the relation

$$\omega_{max} = \frac{6.28}{T_0} \quad \text{rad/s} \tag{5}$$

This relationship may be used to tune the ship motion spectrum in any degree of freedom.

The ship motion response spectrum in any degree of freedom is computed as

$$S_\eta(\omega) = \left|H_\eta(j\omega)\right|^2 \; S_\zeta(\omega) \tag{6}$$

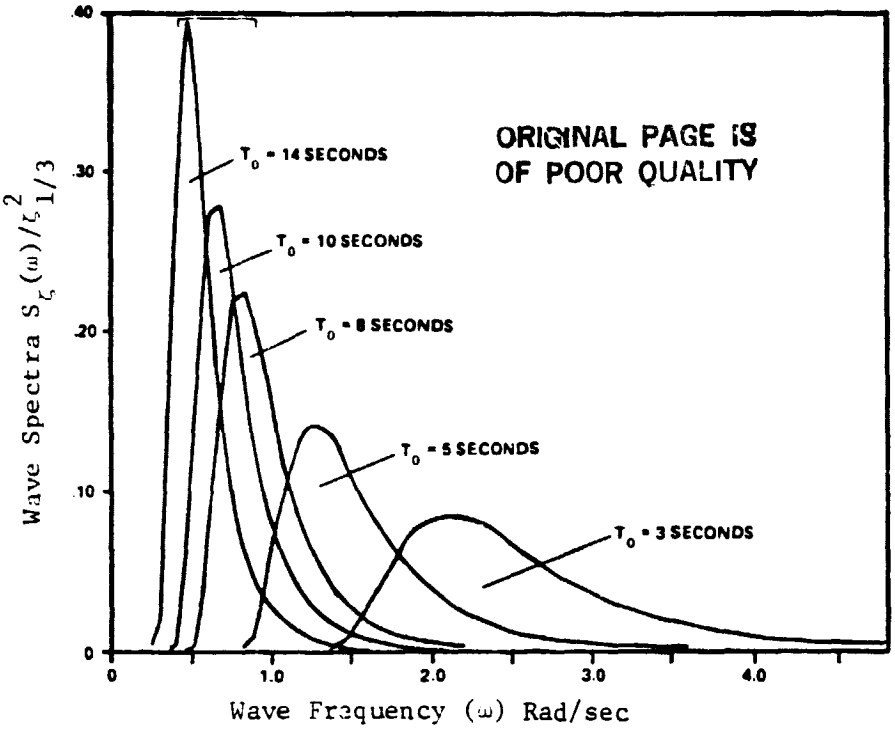

Figure 3. Normalized Bretschneider Spectrum for Varying Modal Period T_0. [From Ref. 1].

In order to compute the response spectrum in the encounter frequency (ω_e) domain, it is necessary to use the mapping

$$\omega_e = f(\omega) = \omega - \frac{\omega^2}{g} V_s \cos \mu_s \tag{7}$$

where V_s = ship speed

μ_s = ship heading with respect to the predominant wave direction

g = acceleration due to gravity (32.2 ft/s^2).

Thus,

$$S_\eta(\omega_e) = \left[\frac{S_\eta(\omega)}{\frac{\partial \omega_e}{\partial \omega}} \right]_{\omega = f^{-1}(\omega_e)}$$

$$= \left[\frac{S_\eta(\omega)}{1 - \frac{2\omega}{g} V_s \cos \mu_s} \right]_{\omega = f^{-1}(\omega_e)} \tag{8}$$

where

$$\omega = f^{-1}(\omega_e) = \frac{-1 + \sqrt{1 + \frac{4\omega_e V_s \cos \mu_s}{g}}}{2 \frac{V_s \cos \mu_s}{g}} \tag{9}$$

Figure 4 illustrates the steps involved in computing $S_\eta(\omega_e)$.

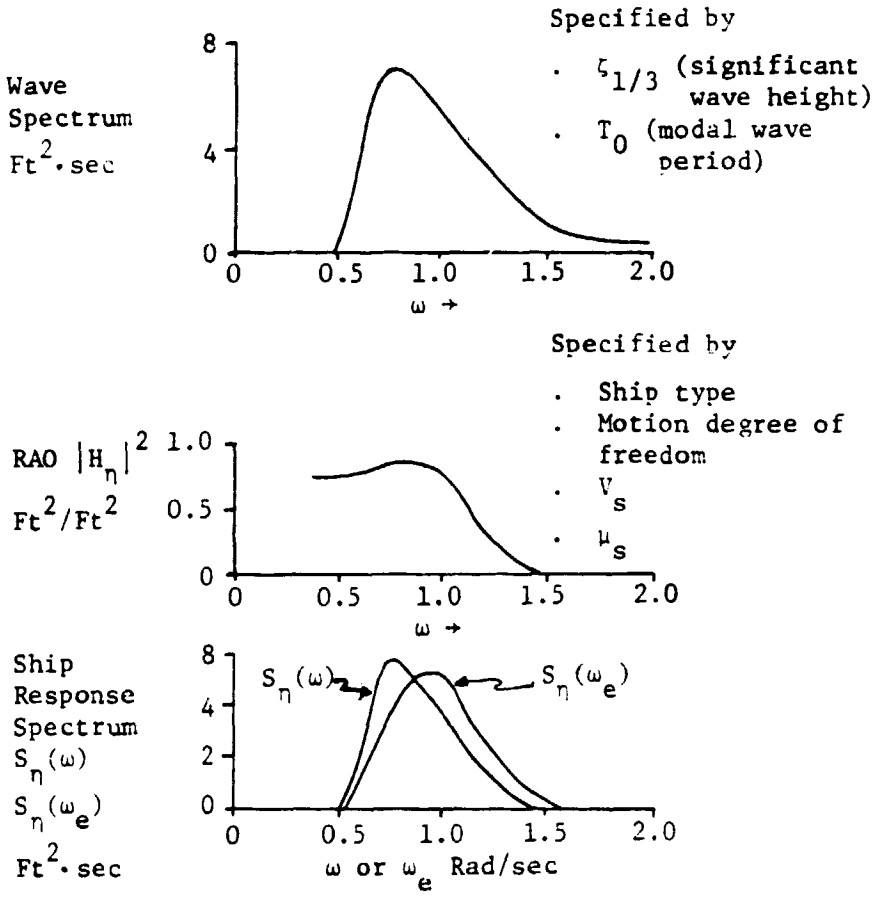

Figure 4. Ship Response Spectrum Computation

In wave theory, the square of the ship transfer function magnitude is called the Response Amplitude Operator (RAO). Thus,

$$RAO_\eta(\omega) = \left|H_\eta(j\omega)\right|^2 \tag{10}$$

RAO data for each of the six degrees of freedom are usually generated by measuring ship response in towing tank experiments or derived computationally by exercising the NSRDC Ship Motion and Sea Load Computer

Program [3]. It should be noted that RAO data depend upon the type of ship, the ship's speed (V_s) and heading (μ_s), and the degree of freedom.

The sum of sinusoids model for describing ship motion time history for any degree of freedom is expressed as:

$$\eta(t) = \sum_{i=1}^{N} \eta_i \cos (\omega_{ei} t - \phi_i + \varepsilon_i) \tag{11}$$

where N = number of sinusoids

ω_{ei} = location of the i th frequency component

$\phi_i = - \underline{|H_\eta(j\omega_i)|}\Big|_{\omega_i = f^{-1}(\omega_{ei})} \equiv \phi_\eta(\omega_i)$

= phase lag of the ship transfer function at the i th frequency

η_i = amplitude of i th frequency component

ε_i = random phase of i th frequency component ~ [0 - 2π]

Note that: $H_\eta(j\omega) \triangleq |H_\eta(j\omega)| e^{j \underline{|H_\eta(j\omega)}}$

$$\equiv \sqrt{RAO_\eta(\omega)}\, e^{-j \phi_\eta(\omega)}$$

The N frequencies ω_{ei} are equispaced $\delta\omega_e$ apart over the encounter frequency range $[\omega_{e\,min}, \omega_{e\,max}]$ where the ship motion spectrum $S_\eta(\omega_e)$ exceeds 4% of its maximum value. The corresponding N amplitudes η_i are chosen such that the power of the sinusoid at ω_{ei} approximates the area under the power spectrum $S_\eta(\omega_e)$ over the frequency bin

$$\left[\omega_{ei} - \frac{\delta\omega_e}{2}, \ \omega_{ei} + \frac{\delta\omega_e}{2}\right].$$

Thus,

$$\frac{\eta_i^2}{2} \triangleq S_\eta(\omega_{ei})\, \delta\omega_e \tag{12}$$

or

$$\eta_i = \sqrt{2\, S_\eta(\omega_{ei}) \cdot \delta\omega_e} \tag{13}$$

Note, however, that the NAEC Ship Motion Computer Program [1] used in this study, performs spectral decomposition into a sum of sinusoids in the wave frequency (ω) domain. In other words, N equispaced frequencies ω_i are selected in the ω domain with η_i computed as

$$\eta_i = \sqrt{2 \cdot S_\eta(\omega_i) \cdot \delta\omega} \tag{14}$$

where $\delta\omega$ is the constant frequency spacing. Note that, η_i calculated using Eq. (14) is identical to that obtained from Eq. (13) with $\delta\omega_{ei}$ substituted for $\delta\omega_e$. These amplitudes $\{\eta_i\}$ are assigned to frequencies $\{\omega_{ei}\}$ in the encounter frequency domain, calculated using the frequency mapping defined in Eq. (7) between ω and ω_e. The incremental frequency bins $\delta\omega_{ei}$ are related to $\delta\omega$ by the nonlinear Jacobian transformation,

$$\delta\omega_{ei} = \left.\frac{\partial\omega_e}{\partial\omega}\right|_{\omega = \omega_i} \cdot \delta\omega \tag{15}$$

Consequently, the frequencies in the ω_e domain are not uniformly spaced. In fact for the case (V_s = 25 kt, μ_s = 120°) considered in this study, the Jacobian $\frac{\partial\omega_e}{\partial\omega}$ over the frequency range of interest is slightly greater than one. The result is a slow rise in bin size $\delta\omega_{ei}$ as i increases from 1 to N. However, for the purpose of this study, this effect was not considered to be serious enough to warrant a modification of the NAEC program.

2.1.1 Generation of Simulated Ship Motion Data

The NAEC Ship Motion Computer Program [1] was used to generate simulated ship motion time histories. However, in order to use the program, it is necessary to specify the following three sets of parameters:

a) ship type, speed V_s and heading μ_s ;

b) sea spectrum parameters - namely, significant wave height $\zeta_{1/3}$ and modal period T_0; and

c) ship dynamics parameters - namely the $RAO_\eta(\omega)$ and phase angles $\phi_\eta(\omega)$ over the frequency range of interest, for each degree of freedom η.

The DD963 Spruance class destroyer data base provided by the NAEC program was used to generate the motion time histories. The program data base covers an operating range of ship speeds V_s from 5 to 25 kt in 5 kt increments, and ship headings from 0 (following seas) to 180 (head seas) in 15 degree increments. Figure 5 shows the parameters characterizing the ship motion relative to the incident wave direction. For the purpose of this study an operating condition corresponding to V_s = 25 kt and μ_s = 120° was selected because it results in large deck motions in all degrees of freedom (in particular, heave and pitch).

The significant wave height $\zeta_{1/3}$ of 32 ft (9.75 m) was chosen to correspond to a high sea state condition. The modal period T_0 was selected by a tuning process as illustrated in Figure 6. The objective of the tuning process was to select a value for T_0 that results in a heave deck motion spectrum having narrow band characteristics that are typical of actual ship motion. Figures 6a and 6b show the peak magnitude normalized sea spectrum, deck heave RAO, and deck heave spectrum for T_0 = 13.5s and 8.48s, respectively. The value of T_0 = 8.48s tunes the peak of the sea spectrum with the peak of the heave RAO, giving rise to a narrow band heave motion spectrum.

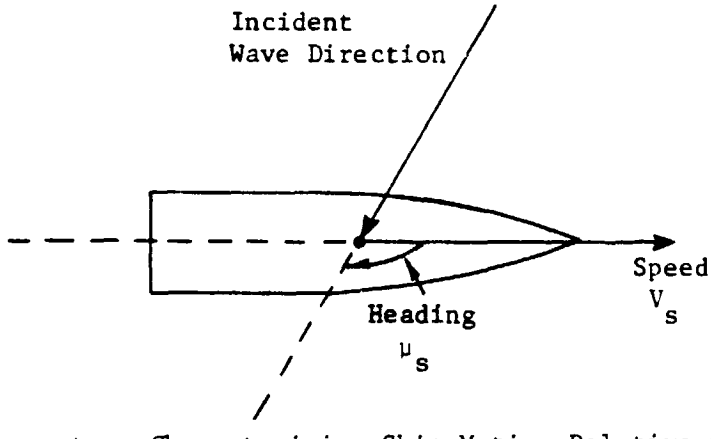

Figure 5. Parameters Characterizing Ship Motion Relative to Incident Wave Direction.

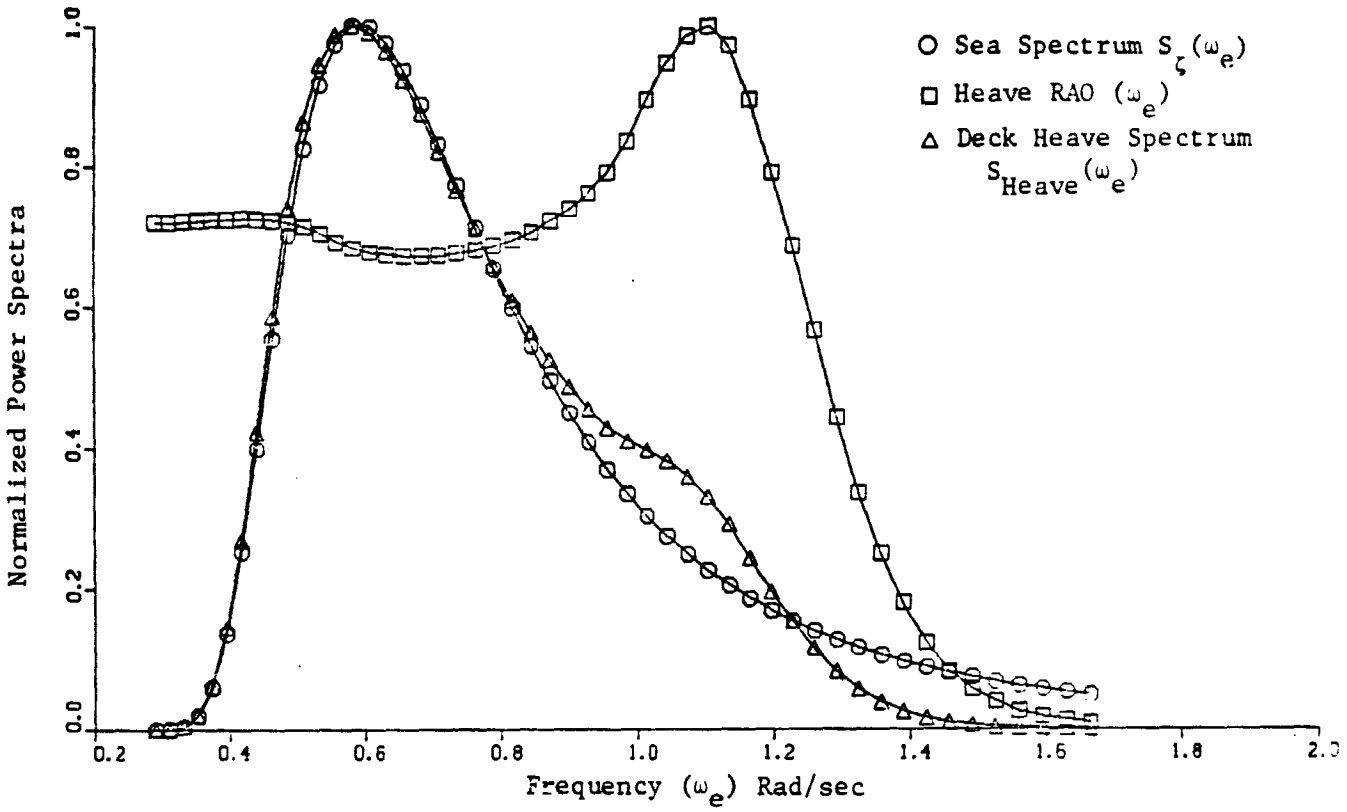

a) T_0 = 13.5 s

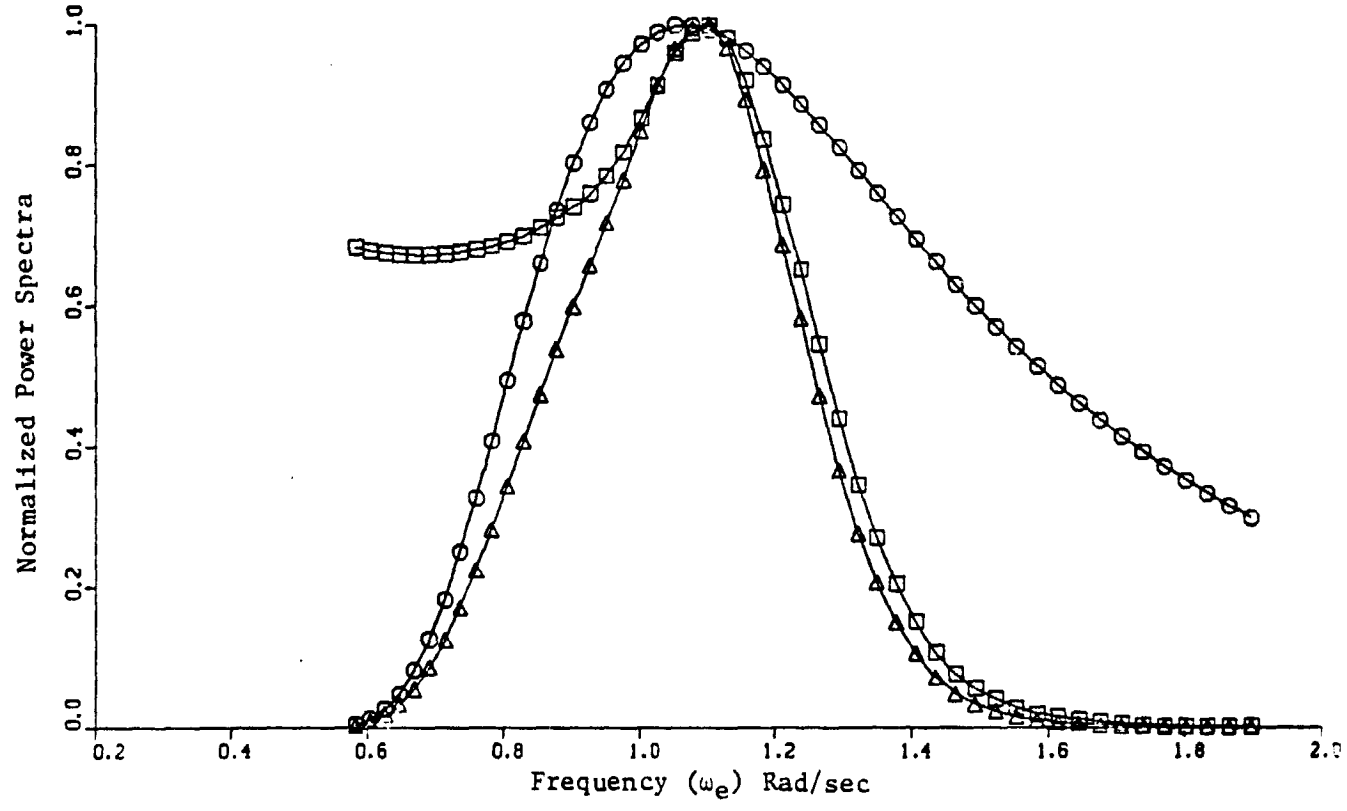

b) T_0 = 8.48 s

Figure 6. Tuning Process in the Selection of the Modal Period T_0.

Figure 7 shows the simulated DD963 ship motion time histories using a sum of seventy sinusoids over a 1200s interval for the six deck motion degrees of freedom. The motion is described in a local level reference frame centered at the average position of the bullseye, with x axis astern, y axis starboard and z axis up. The deck motion quantities shown are:

$$
\begin{aligned}
x &- \text{longitudinal} \\
y &- \text{lateral} \\
z &- \text{heave or vertical} \\
\phi &- \text{roll} \\
\theta &- \text{pitch} \\
\psi &- \text{yaw}
\end{aligned}
\tag{16}
$$

The ordinate scales for dimensionally equivalent translational and rotational quantities are identical to facilitate visual comparison of their relative magnitudes and temporal characteristics. Examination of these time histories reveals that the motions display temporal characteristics that are typical of narrow-band random processes. Specifically, the time histories show an alternating sequence of quiescent and large ship motions, referred to in the literature as lulls and inter-lulls (or swells) [4]. Furthermore, it appears that the lulls and inter-lull intervals are synchronized across the six degrees of freedom.

However, previous work by Fortenbaugh [5] concluded that a sum of six sinusoids (N = 6) should provide an excellent approximation for representing actual ship motions. This conclusion was based on showing that root-mean-square (rms) position, rate, and acceleration for each of the six degrees of freedom differ by less than 5% for the six or thirty-two sinusoids approximations. This agreement of rms values does not guarantee equivalence of the underlying distributions, correlation functions, and simulated time histories of the motion in each degree of freedom. This is apparent on a cursory examination of the time histories for $[\phi, \dot{\phi}, \theta, \dot{\theta}, z, \dot{z}]$ for the six and seventy sum of sinusoids models, shown in Figures 8 and 9, respectively. Most importantly, the time histories (Fig. 8) for the sum of six sinusoids do not display the alternating lull and swell periods so obvious in the seventy sinusoids model (Fig. 9 and Fig. 7). Furthermore, the six sinusoids data has a

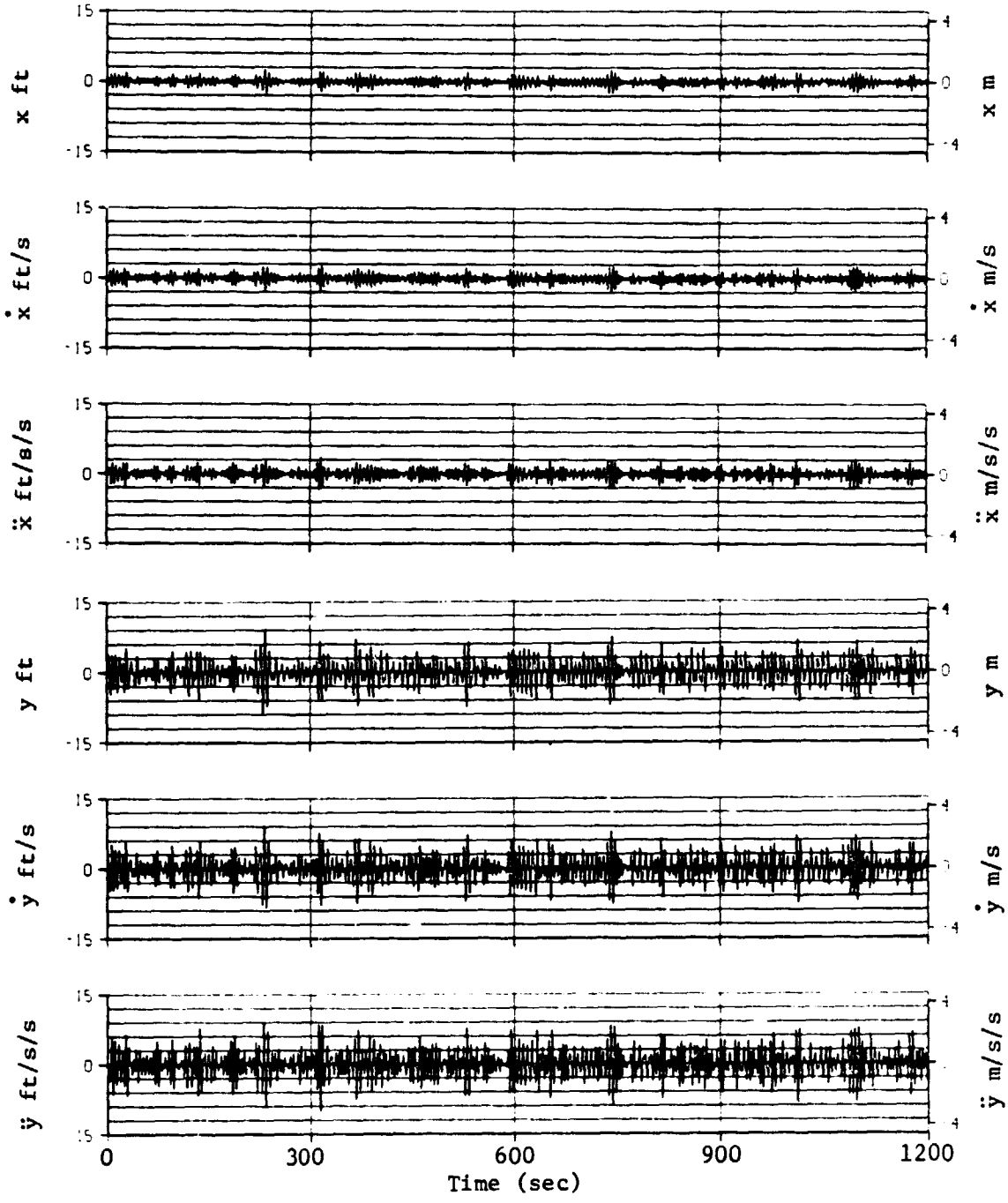

Figure 7. Simulated Ship Motion Time Histories (70 Sinusoids): V_s = 25 kt, μ_s = 120°, $\zeta_{1/3}$ = 32 ft, T_0 = 8.48 s.

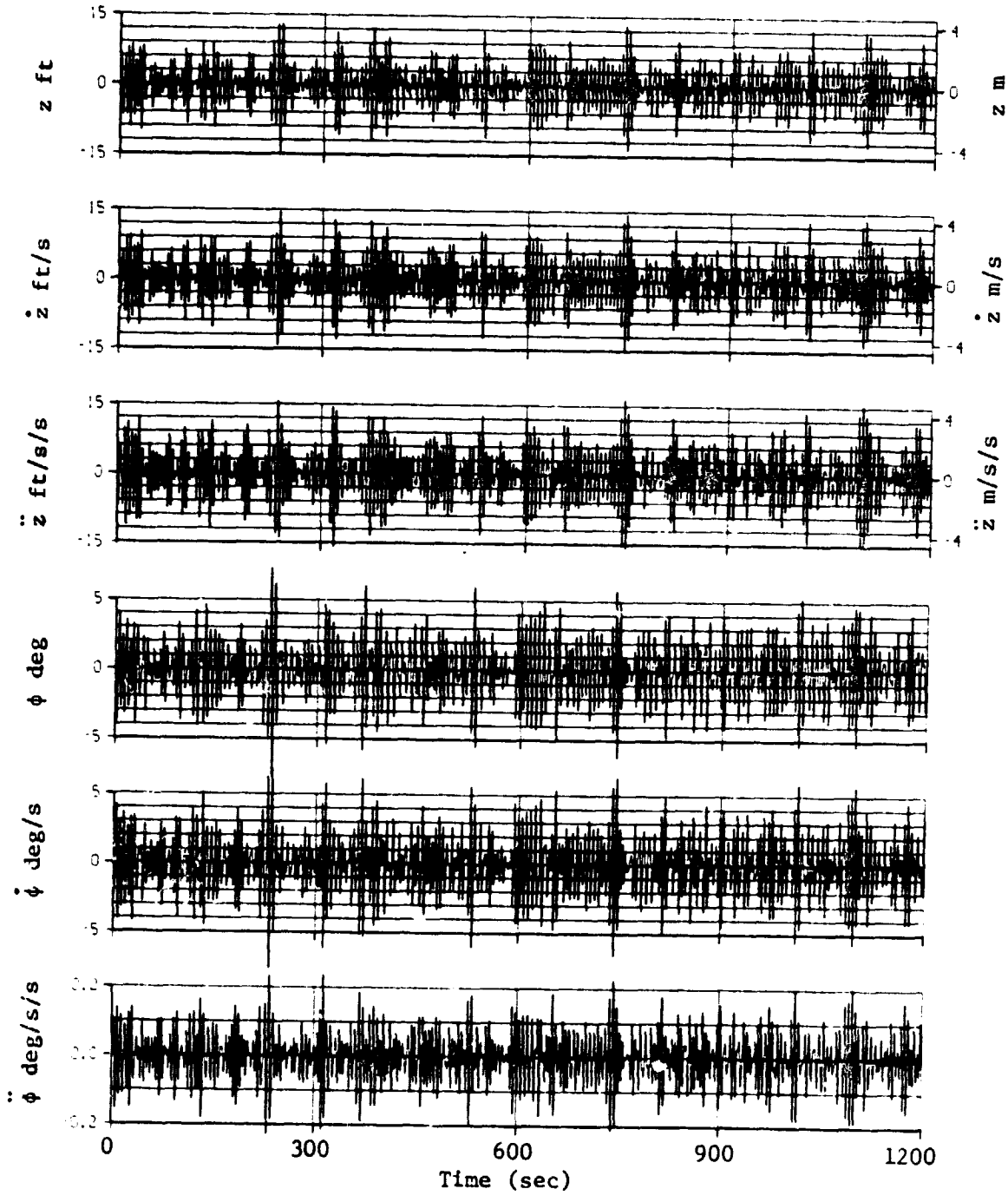

Figure 7. (Cont.)

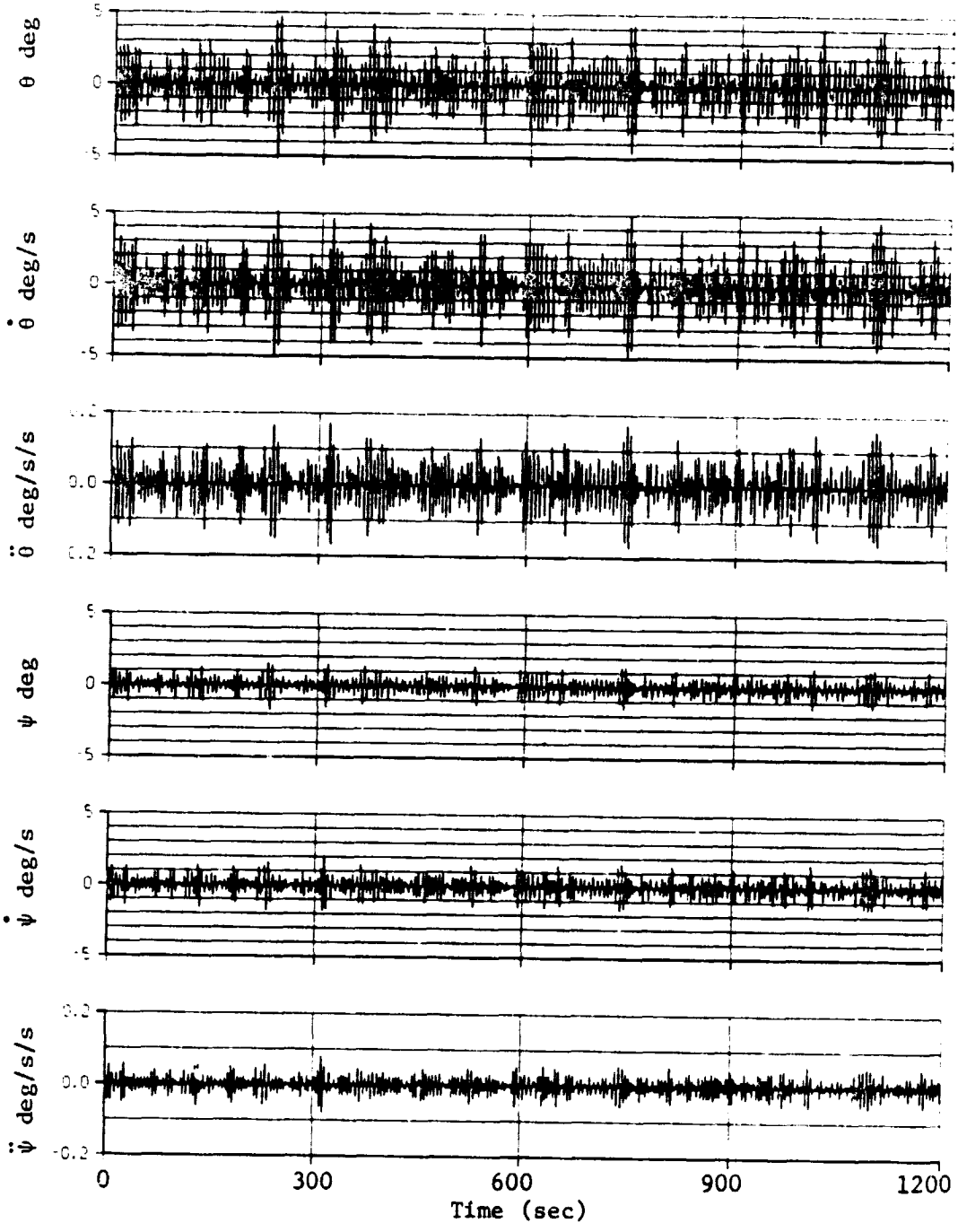

Figure 7. (Cont.)

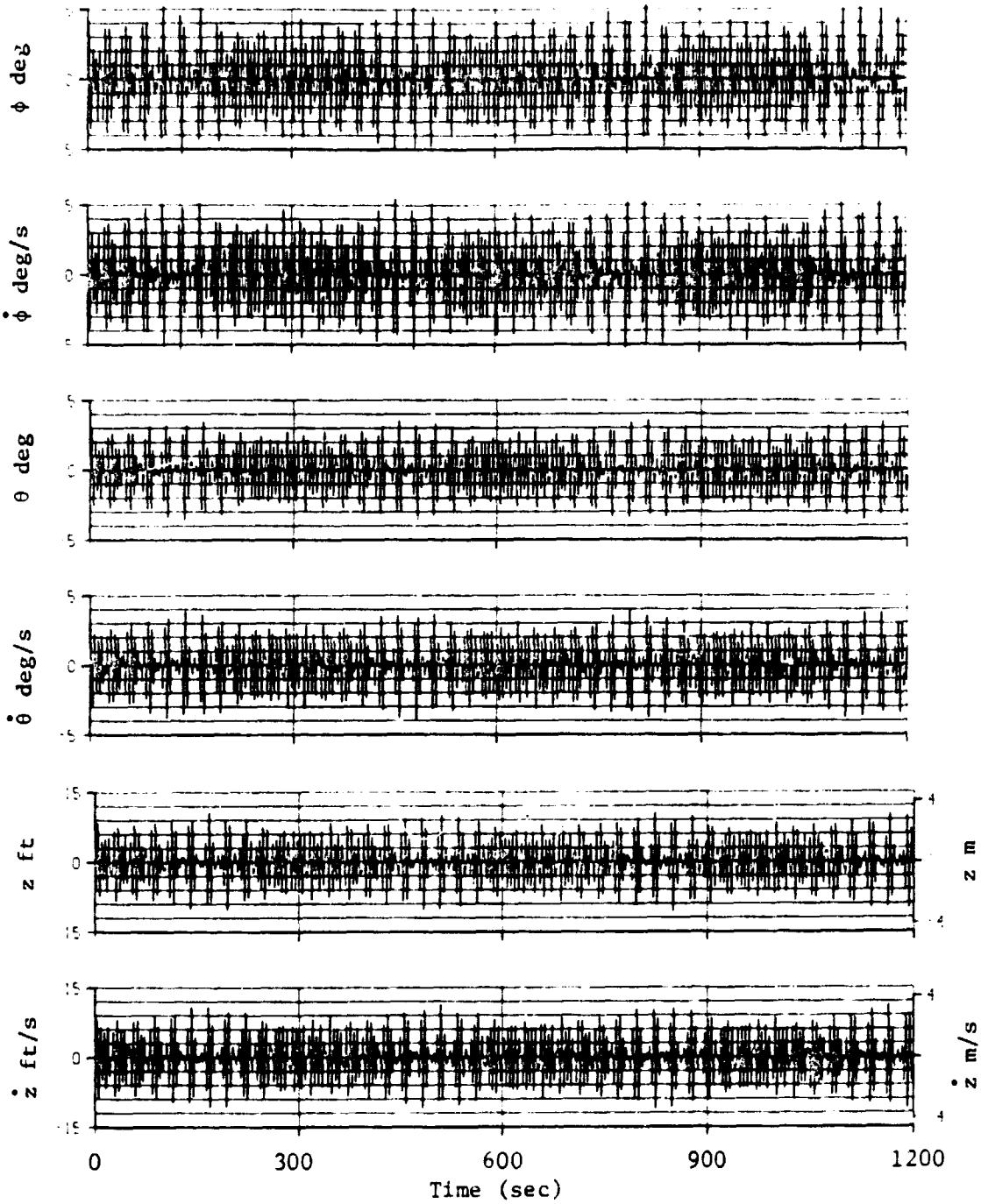

Figure 8. Simulated Ship Motion Time Histories (6 Sinusoids): V_s = 25 kt, μ_s = 120°, $\zeta_{1/3}$ = 32 ft, T_0 = 8.48 s.

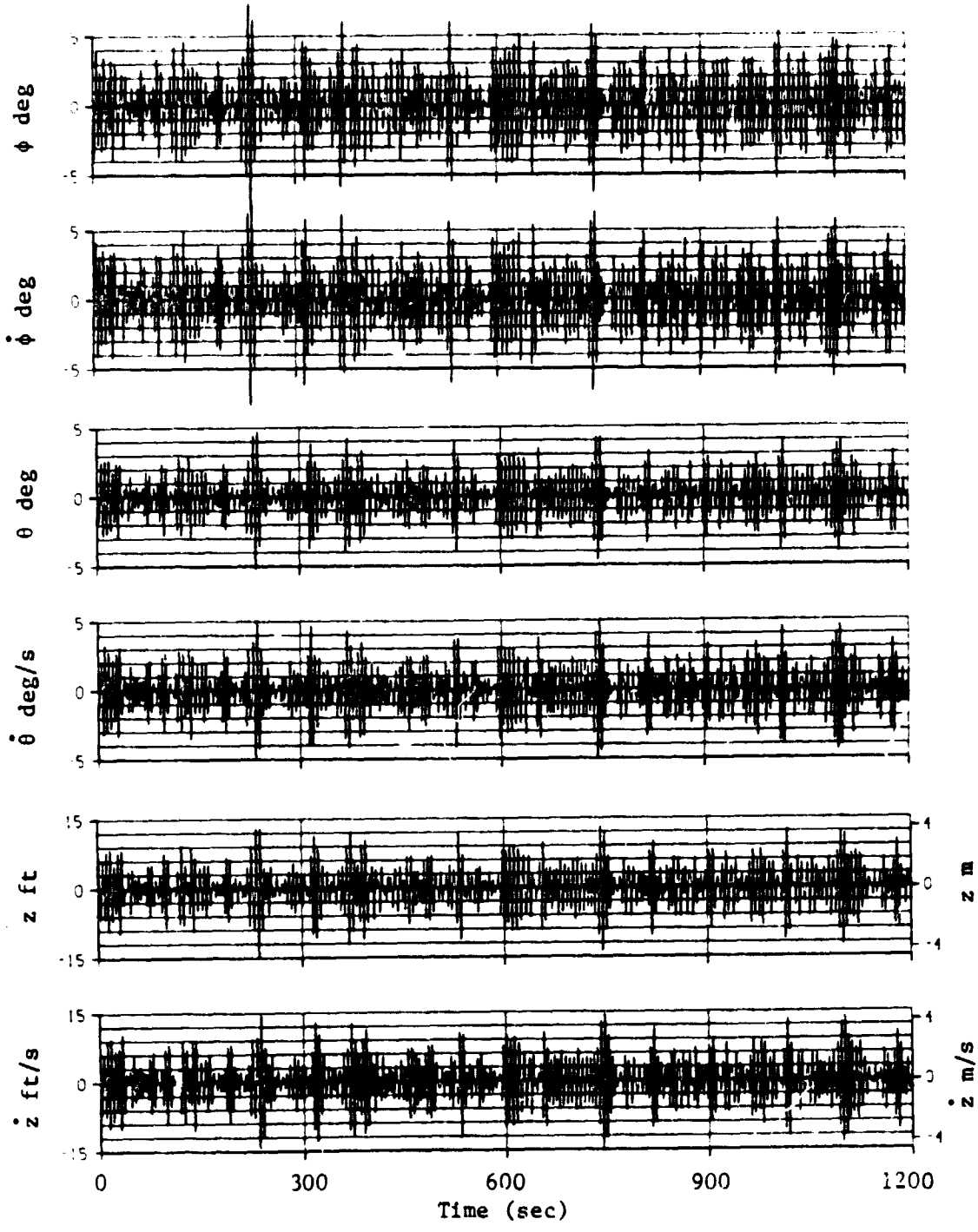

Figure 9. Simulated Ship Motion Time Histories (70 Sinusoids): V_s = 25 kt, μ_s = 120°, $\zeta_{1/3}$ = 32 ft, T_0 = 8.48 s.

definite repetitive pattern with a fundamental period of approximately 340 seconds. Differences in the underlying distributions for the two cases are also noticeable in the histograms for deck heave (z) and vertical velocity ($\dot{z}$) shown in Figure 10. The sum of seventy sinusoids distributions are markedly more Gaussian than the ones for six sinusoids, the most noticeable discrepancy being in the six sinusoids histogram for $\dot{z}$. The whole issue of developing minimal complexity models (including, but not limited to sum of sunusoids or state-space models) for real time ship motion simulation is an interesting area for more systematic research but was considered to be outside the scope of this study effort.

Henceforth, ship motion data generated by the NAEC Ship Motion Computer Program using a sum of seventy sinusoids representation (see sample time histories in Figure 7) will be used as a baseline for investigating shipboard landing guidance system concepts.

2.2 Landing Envelope Definition

Landing envelope is a term used to define the acceptable set of conditions at touchdown. Typically, these requirements are stipulated in terms of the aircraft state $\underline{x}_A$, the landing pad state $\underline{x}_P$, and the relative state of the aircraft with respect to the pad $\underline{x}_{A/P} (\triangleq \underline{x}_A - \underline{x}_P)$ at touchdown. Note that the state vector is assumed to be composed of the three position (x,y,z) and three attitude (ψ,θ,ϕ) components, and their first and second derivatives. Thus, given the constraints on $\underline{x}_A$, $\underline{x}_P$ and $\underline{x}_{A/P}$ as

$$\underline{x}_A \in S_A \tag{17}$$

$$\underline{x}_P \in S_P \tag{18}$$

and

$$\underline{x}_{A/P} \in S_{A/P} \ , \tag{19}$$

where "$\in$" means "belongs to" or "is a member of" and "S" denotes a "set" in state-space coordinates.

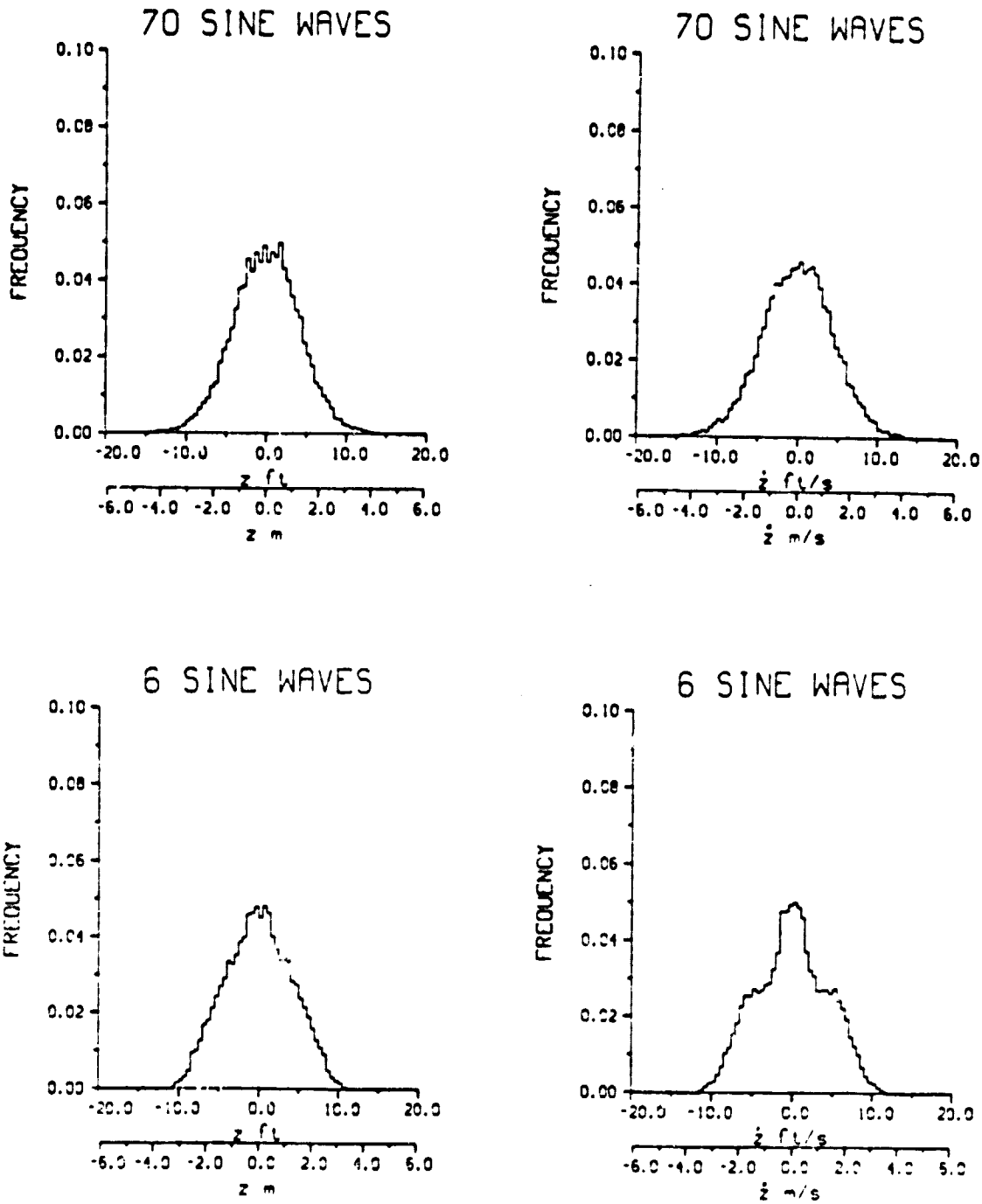

Figure 10. Probability Density Functions for z and $\dot{z}$ for Sum of 70 and 6 Sinusoids.

the landing envelope E is defined as the set of aircraft and landing pad states satisfying Eq. (17)-(19). Thus,

$$E \triangleq \left\{ \underline{x}_A, \underline{x}_P : \underline{x}_A \in S_A \text{ and } \underline{x}_P \in S_P \text{ and } \underline{x}_{A/P} \in S_{A/P} \right\} \tag{20}$$

A review of previous work on the shipboard landing problem indicates that there is no consistent definition of a landing envelope in the sense defined by Eq. (20). However, it is generally agreed that, as a minimum, the relative attitude and translational velocity of the aircraft with respect to the landing pad at touchdown should be within reasonable bounds. For example, at the time of touchdown, conditions such as the following may be stipulated:

$$\begin{aligned}
\phi_{A/P} &\leq \phi_{max} \\
\theta_{A/P} &\leq \theta_{max} \\
\psi_{A/P} &\leq \psi_{max} \\
\dot{x}_{A/P} &\leq \dot{x}_{max} \\
\dot{y}_{A/P} &\leq \dot{y}_{max} \\
\dot{z}_{A/P} &\leq \dot{z}_{max}
\end{aligned} \tag{21}$$

Unanimity on selection of the numerical values for these limits is not possible because of their dependence on ship type, aircraft landing gear characteristics and other operational factors. Additional limits on landing pad state at touchdown are usually imposed because of limitations in the aircraft control power (thrust/weight ratio), and the speed of response (i.e. bandwidth) of the attitude and vertical translational flight control systems. These aircraft bandwidth limitations preclude the design of a ship motion following landing control system during constant speed letdown. As a result, previous studies [6-8] have proposed the following requirements on the landing pad motion at touchdown:

a) The pad vertical position with respect to its average value shall be greater than zero.

$$\text{i.e.:} \quad z > 0 \tag{22}$$

b) The vertical velocity of the pad shall be positive (moving upward) but shall be less than some prescribed value (e.g. .6 m/s or 2 ft/s)

$$\text{i.e.:} \quad 0 < \dot{z} \leq \dot{z}\Big|_{max} \tag{23}$$

c) The pitch and roll attitudes and rates shall be less than some prescribed values

$$\text{i.e.:} \quad \begin{aligned} |\theta| &\leq \theta\Big|_{max} \\ |\dot{\theta}| &\leq \dot{\theta}\Big|_{max} \\ |\phi| &\leq \phi\Big|_{max} \\ |\dot{\phi}| &\leq \dot{\phi}\Big|_{max} \end{aligned} \tag{24}$$

Equations (22)-(24) represent one plausible set S_p (see Eq. 18) of acceptable landing pad states at touchdown, and provide an example for elucidating the underlying concept. These three constraints reflect a conservative landing guidance philosophy where the landing window is limited to periods during which the ship's landing pad motion is small and at its peak or crest values. There restrictions are imposed to minimize the probability of large heave velocity at touchdown thereby reducing the chances for a hard landing.

The basic objective of landing guidance is to bring the aircraft to a safe touchdown onboard the deck while staying within its control system limitations. A careful review of previous work on the subject indicates little agreement on the parameters defining an acceptable landing envelope. As a result, a normative approach is used in this study towards evaluating alternative landing guidance systems concepts, whereby improvements in touchdown performance obtained with alternate designs are normalized with respect to the performance of a simple constant-rate-of-descent letdown controller.

The simplest form of letdown procedure is to use no active guidance by allowing constant rate-of-descent to a touchdown at any time after the aircraft has achieved a stable hover position over the ships landing pad. The touchdown performance achieved with the CROD letdown profile may, therefore, be examined to establish a baseline or standard of performance against which alternative letdown guidance schemes may be measured.

Figure 11 illustrates the CROD letdown scenario. Throughout the remainder of this report, the stationkeeping or hover point is assumed to be at a constant altitude of 20 ft over the average position of the bullseye. This height was chosen to allow a safe clearance above the maximum deck height (≈ 15 ft) obtained under the simulated landing conditions (i.e., V_s = 25 kt, μ_s = 120°, $\zeta_{1/3}$ = 32 ft, T_0 = 8.48 s).

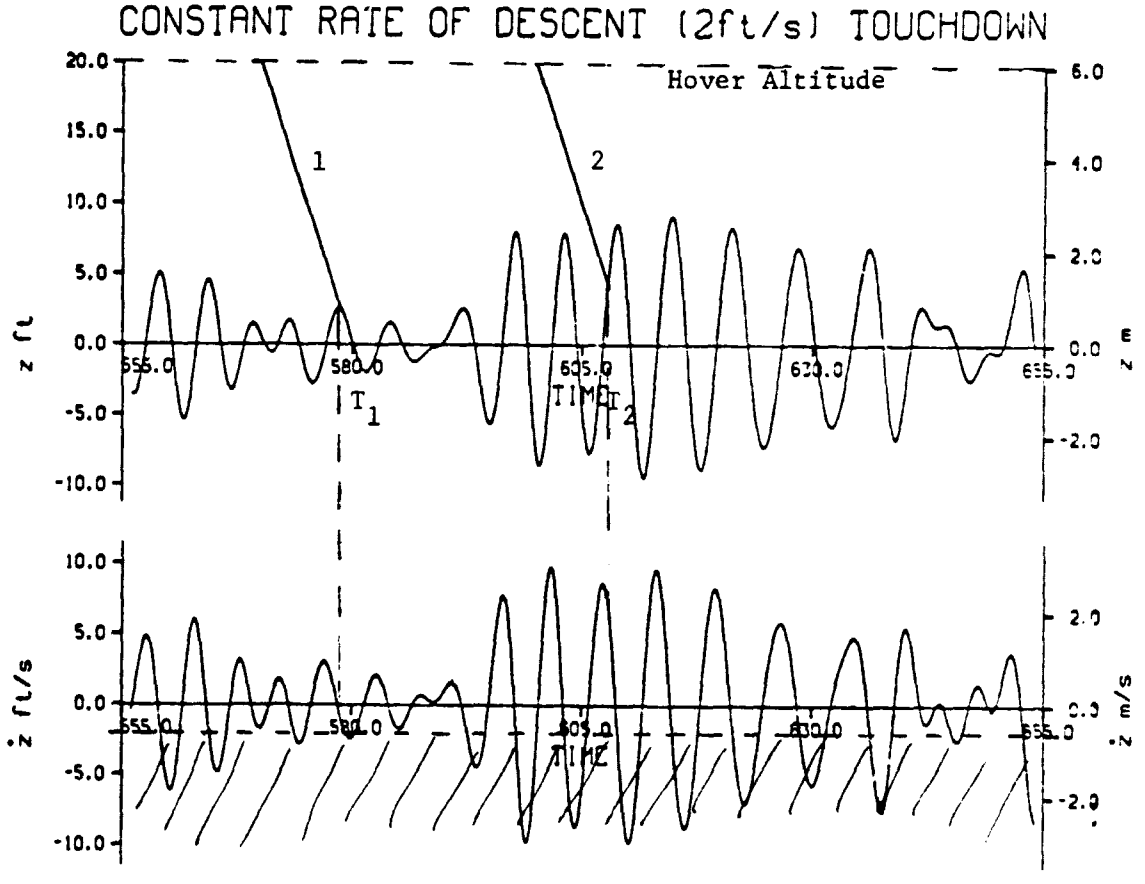

Figure 11. Constant Rate of Descent (2 ft/s) Letdown.

Note that for a 2 ft/s letdown rate, touchdowns occur only when pad vertical velocity is greater than -2 ft/s (i.e. above the cross-hatched region in $\dot{z}$). Since the principal factor limiting shipboard landing is the relative vertical impact velocity between the aircraft landing gear and the ship's deck at touchdown, only the landing pad vertical motion (z) and vertical velocity ($\dot{z}$) are shown over a 100 second segment. Two CROD (2 ft/s) letdown profiles are illustrated. The figure shows that profiles 1 and 2 land during different periods of ship motion. Letdown profile 1 lands ($T_1 \tilde{=} 578$s) when ship motion is in a relatively quiescent period while profile 2 touches down ($T_2 \tilde{=} 608$ s) during large amplitude period. As a result, the touchdown vertical impact velocity is 1 ft/s for profile 1 and 8 ft/s for profile 2. The CROD letdown is performed with the aircraft attitude at trim value (assumed to be zero attitude throughout this report i.e. $\psi_A = \theta_A = \phi_A = 0°$). Therefore, touchdown performance in the remainder of the translational (i.e. x, $\dot{x}$, $\ddot{x}$, y, $\dot{y}$, $\ddot{y}$) and rotational (ϕ, $\dot{\phi}$, $\ddot{\phi}$, θ, $\dot{\theta}$, $\ddot{\theta}$, ψ, $\dot{\psi}$, $\ddot{\psi}$) variables may be expressed directly in terms of the landing pad conditions at touchdown.

Touchdown performance can be evaluated by examining the histograms (or probability density functions - PDF's), cumulative distribution functions (i.e. $F(x) = \Pr[X \leq x]$) or survival functions (i.e. $\mathcal{F}(x) = \Pr[X > x] = 1 - \Pr[X \leq x] = 1 - F(x)$) for the individual variables. A Monte Carlo simulation approach was used in this study to compute the touchdown statistics. The simulation allowed for a letdown profile to be initiated every 1 second. Touchdown data over a one hour period (approximately 3600 touchdowns)were used to compute the histograms and distributions of the individual state variables. An examination of the ship motion time histories in Figure 7 indicates that out of the eighteen variables shown, only four, namely $\dot{z}$, $\dot{y}$, $\ddot{y}$ and $\dot{\phi}$, may be limiting factors in achieving an acceptable touchdown performance. Therefore, discussion of the results will be limited to these four quantities. Touchdown performance will be characterized in terms of survival functions for the vertical impact velocity $\dot{z}_R (\equiv \dot{z} - \dot{z}_A)$, lateral impact velocity $\dot{y}$, lateral

impact acceleration $\ddot{y}$ (proportional to side force on landing gear), and roll angular velocity $\dot{\phi}$. Plots for survival function are given for $\dot{z}_R$, alone. However, survival function results in a tabular format are provided for each of the four variables. Note that the survival function gives the probability of a given variable exceeding a prescribed threshold. This function, therefore, provides a direct measure of the touchdown performance in concrete and tangible terms.

The survival function, $\mathscr{F}(\dot{z}_R)$, for the 2 ft/s CROD letdown guidance scheme is shown in Figure 12. Corresponding results for $\dot{z}_R$, $|\dot{y}|$, $|\ddot{y}|$ and $|\dot{\phi}|$ are given in a tabular form in Table 1. Note that an absolute value on $\dot{z}_R$ is not necessary since $\dot{z}_R \geq 0$, by definition. Note that

$$\mathscr{F}(|\dot{y}|) \triangleq \text{Probability that absolute lateral impact velocity at touchdown is greater than } |\dot{y}| \qquad (25)$$

The same definition applies to $\mathscr{F}(|\ddot{y}|)$ and $\mathscr{F}(|\dot{\phi}|)$. Touchdown performance results for the CROD letdown profile summarized in Table 1 shall be used throughout the remainder of this report for evaluating, on a normative basis, the improvements over CROD guidance provided by alternative letdown schemes.

2.4. Alternative Letdown Guidance Concepts

The performance of a CROD letdown scheme is summarized by the results in Table 1. The purpose of this section is to discuss alternative letdown guidance concepts which give improved touchdown performance by decreasing the probability of touchdowns with large translational and rotational velocities and accelerations at impact.

Two categories of letdown guidance laws may be formulated:

1) Designs based upon the assumption that ship motion response time histories display a pattern of alternating low amplitude quiescent periods called "lulls" followed by large motion inter-lull segments called "swells", and

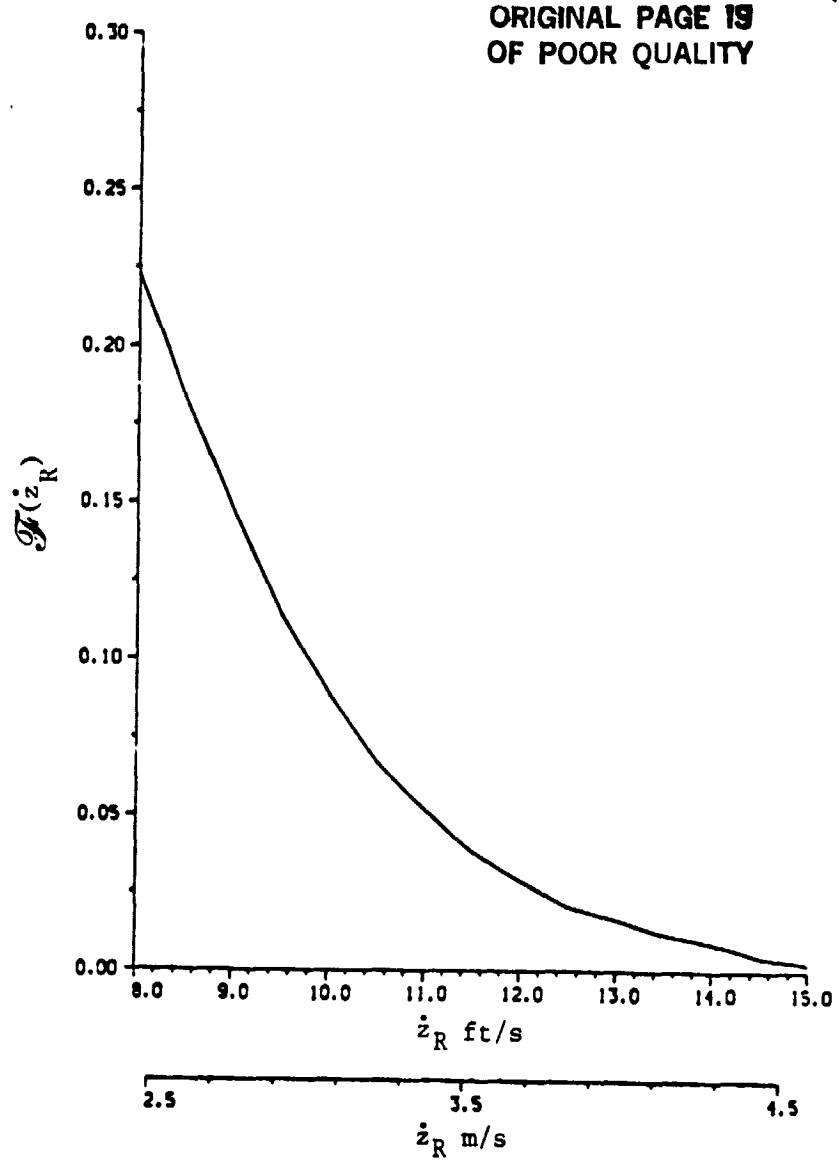

Figure 12. Survival Function $\mathscr{F}(\dot{z}_R)$ for CROD Letdown.

TABLE 1.

CROD Letdown Touchdown Performance

$\dot{z}_R$		$\dot{\phi}$		$\dot{y}$		$\ddot{y}$	
$\dot{z}_R$ (ft/s)	$\mathcal{F}(\dot{z}_R)$ x 100%	$\lvert\dot{\phi}\rvert$ (deg/s)	$\mathcal{F}(\lvert\dot{\phi}\rvert)$ x 100%	$\lvert\dot{y}\rvert$ (ft/s)	$\mathcal{F}(\lvert\dot{y}\rvert)$ x 100%	$\lvert y\rvert$ ft/s/s	$\mathcal{F}(\lvert\ddot{y}\rvert)$ x 100%
6	44	2	44	2	54	2	43
8	22	3	23	4	19	4	12
10	9	4	10	5	9	5	5
12	3	5	3	7	2	7	1

2) Designs that are independent of the presence or absence of a ship motion pattern structure (i.e. lulls and swells).

Previous studies [6-8] of the shipboard landing problem have ignored the existence of ship motion lulls (i.e. design option #1) and have instead proposed two approaches to letdown guidance: A ship motion following controller and a ship motion forecasting controller. The CROD letdown does not allow the aircraft to respond to instantaneous ship motion, and in particular, to its relative attitude and vertical velocity with respect to the moving landing pad. One approach to reducing the relative motion at touchdown is to design a flight control system or landing controller that forces the aircraft to track or follow the instantaneous landing pad motion while maintaining a CROD letdown until touchdown. The basic idea is illustrated in Figure 13 which shows the application of ship motion following letdown guidance to the vertical motion degree of freedom.

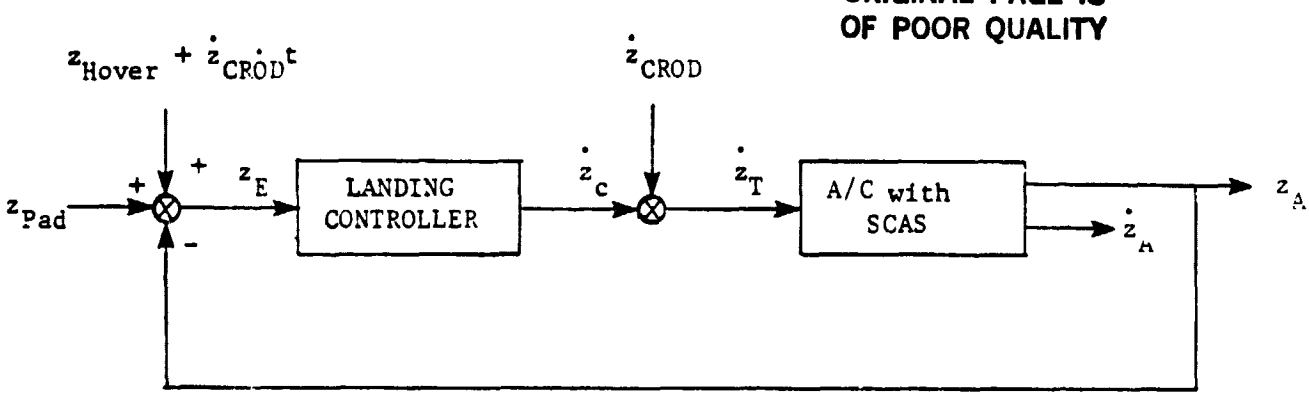

Figure 13. Ship Motion Following Letdown Guidance for Vertical Motion.

Typical response of this design is illustrated in Figure 14. The total vertical velocity command $\dot{z}_T$ is the sum of the nominal CROD command

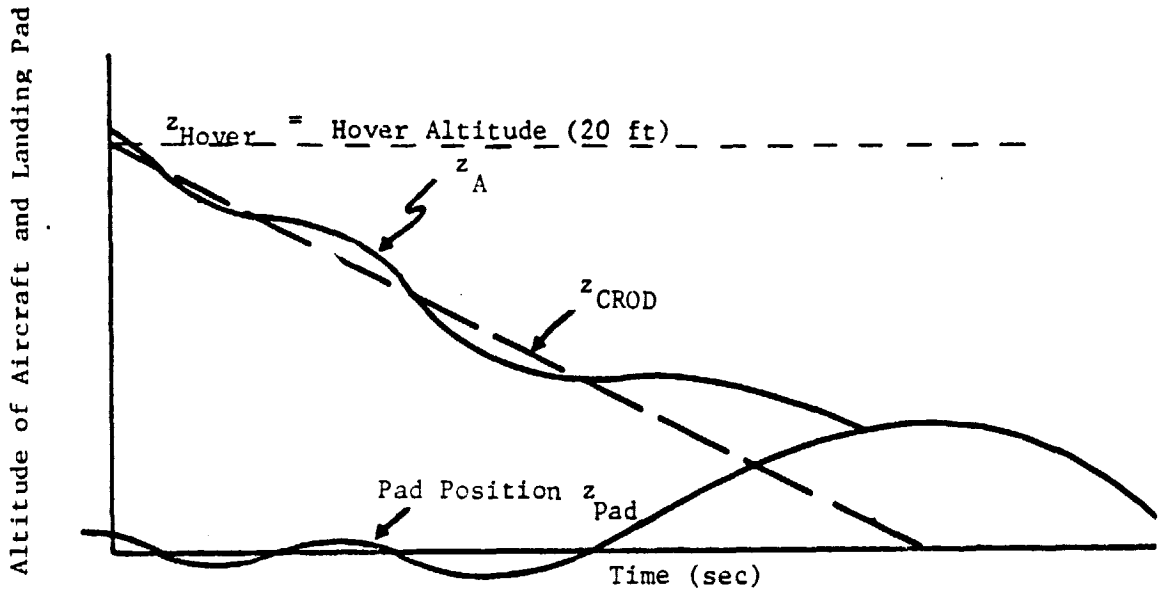

Figure 14. Response of Vertical Ship Motion Following Controller.

$\dot{z}_{CROD}$ ($\equiv$ - 2 ft/s) and a feedback control $\dot{z}_c$. Thus,

$$\dot{z}_T = \dot{z}_{CROD} + \dot{z}_c \tag{26}$$

The command $\dot{z}_c$ is provided by a landing controller whose goal is to minimize the instantaneous position and velocity errors in following vertical ship motion z. The ship motion following landing controller may be designed using classical and/or modern control theory methods; the choice depending upon the nature and quality of the apriori information (i.e. mathematical models for the aircraft, landing pad motion and external gust disturbances). Such a letdown controller can be used only if the aircraft can follow the landing pad motion with reasonable fidelity. This would require a flight control system with a sufficiently high bandwidth (at least three times the dominant frequency in the given ship degree of freedom), servo actuator velocity and acceleration authority limits for successful implementation. However, existing aircraft do not have such characteristics and hence are not capable of following the relatively high frequency (0.3 ~ 2.0 rad/s) deck motions. As a result, ship motion following letdown guidance is not considered to be a viable technique for shipboard landing [8].

An alternative approach is to use some kind of ship motion forecasting algorithm to determine the predicted time periods or landing windows during which aircraft landings would be acceptable. A suitable letdown guidance scheme (e.g. CROD or LQG control with terminal constraints [7]) may be used to bring the aircraft to an acceptable touchdown during the designated landing window. The specific criteria for designating a future time period as a landing window would depend upon the touchdown requirements stipulated by the acceptable landing envelope. However, developing a reliable ship motion forecasting algorithm is a non trivial problem because the efficacy of forecasting methods is predicated upon the veracity of analytical models (e.g. finite order state space or auto-regressive-moving average (ARMA) formulations) used to represent the ship motion spectra (auto and cross spectra). Although the subject of time

series forecasting has received considerable attention over the years [9], and continues to be an area of ongoing research, the usefulness of the available model-based techniques for extrapolation or forecasting of real (as opposed to computer generated) time series is, at best, questionable. Models for ship motion response need to be developed and validated using systematic structure determination and parameter identification techniques with real data obtained from sea trials. However, it must be emphasized that even with exact models for given time series data, the time window over which forecasts can be made with a high level of confidence is finite and limited due to the stochastic nature of the underlying processes.

A ship motion pattern directed letdown guidance scheme was developed in this study. The approach exploits the fundamental temporal characteristic of alternating lull/swell patterns so evident in actual ship motion data and the sum of seventy sinusoids representation of Figure 7. A real time algorithm for lull/swell classification based upon ship motion pattern features is described in the next section. The output of the classification algorithm is used to command a go/no go signal to indicate the initiation and termination of a landing window. Performance improvements obtained with such a go/no go pattern based letdown guidance scheme are discussed in section 4.

3. SHIP/LANDING PAD MOTION PATTERN ANALYSIS

Ship motion response time histories as shown in Figure 7, can be classified into one of two categories or modes: (1) a "lull" mode representing time intervals where overall ship motion may be described as relatively low, and (2) a "swell" mode where ship motion is relatively high. Since the lulls and swells for all the six degrees of freedom appear to be synchronized, any one of the eighteen variables in Figure 7 may be used for lull/swell categorization. In this effort, the landing pad vertical motion z(t) was used to develop a real time lull/swell classification algorithm.

The concept of a lull is best described by reference to Figure 15 where the top two plots (a) and (b) show sample landing pad vertical position z(t), and velocity $\dot{z}(t)$, over a one hundred second interval (identical to z and $\dot{z}$ in Figure 11). The lull/swell classification algorithm is characterized by an indicator function I(z) which maps the ship motion z(t) (including, if necessary, higher derivatives $\dot{z}$ and $\ddot{z}$) into a binary output sequence of zeros and ones, where I(z) = 0 corresponds to a lull period and I(z) = 1 describes an inter-lull interval or swell. An examination of the vertical motion time histories (i.e., z, $\dot{z}$, $\ddot{z}$) in Figure 15 (and Figure 7 for a 1200 second period) shows that the most obvious way to dichotomize the motion into lulls and swells is by defining an indicator function in terms of a threshold amplitude z_T, such that

$$I(z) \equiv I_z \triangleq \begin{cases} 0 \text{ (Lull)}: z(t) \leq z_T \\ 1 \text{ (Swell)}: z(t) > z_T \end{cases} \tag{27}$$

However, the lull/swell switch plots I_z that are obtained using this definition display a high switching frequency (0 to 1 and vice versa) making such a criterion unacceptable from a practical viewpoint. The reason for this behavior is the existence of a relatively large number of single peaks in z(t) exceeding (below) the threshold z_T that occur during otherwise long periods, where $z(t) \leq z_T$ ($z(t) > z_T$). The net result is a large number of lulls and swells of extremely small duration ($\leq$ 3 s)

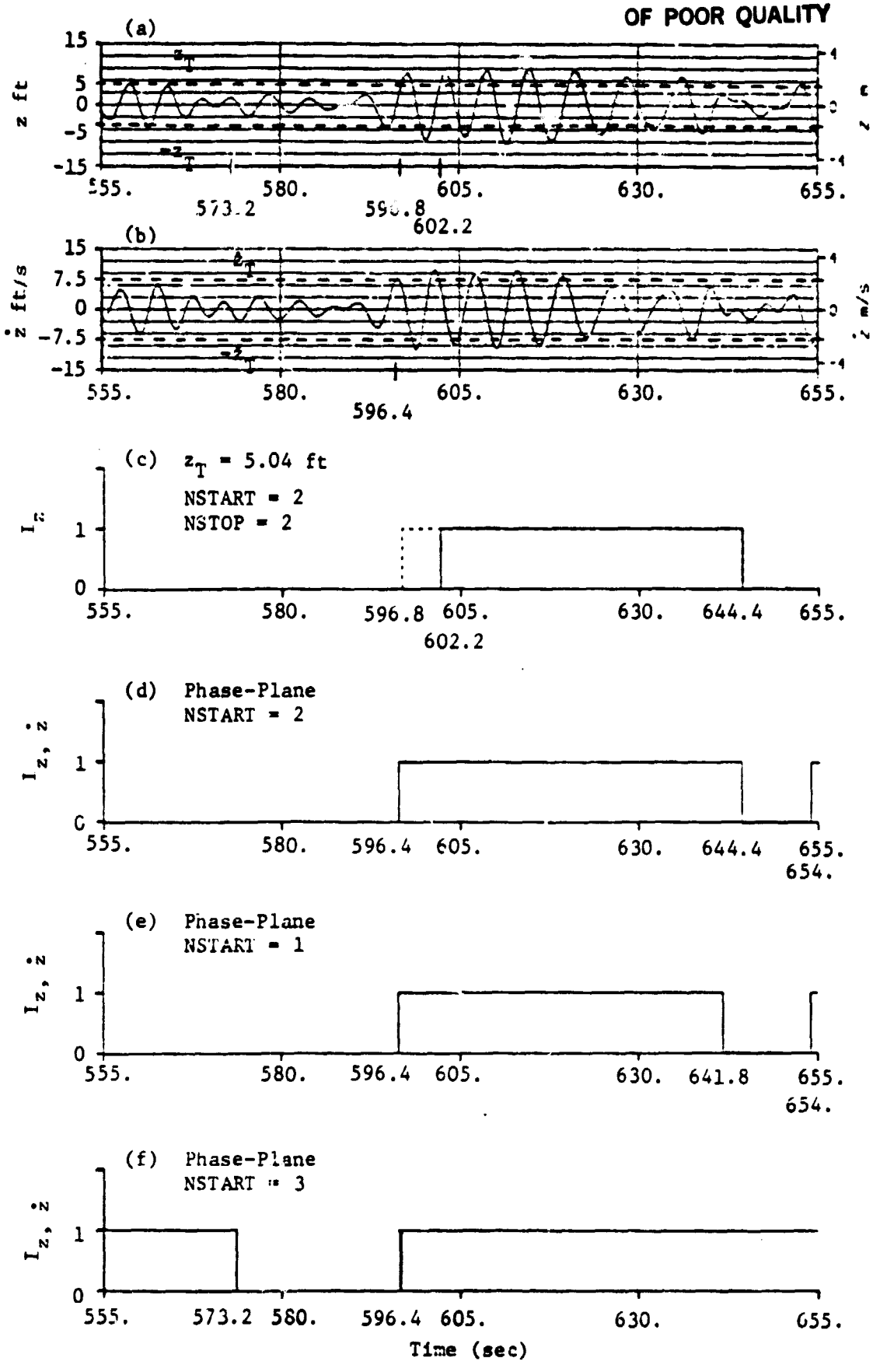

Figure 15. Lull/Swell Classification Algorithm.

that are imbedded in relatively longer duration swell and lull intervals.

A more reasonable approach is to define the initiation and termination of a lull in terms of parameters that reflect the motion response characteristics over a finite past or memory interval. Thus, initiation of a lull may be defined by a parameter "NSTART" as follows. A lull is said to begin (i.e.: I_z switches from 1 to 0) if NSTART consecutive positive peaks of z(t) fall below a prescribed threshold value z_T. Similarly, termination of a lull (or onset of a swell) may be defined by a parameter "NSTOP" as follows. A lull is said to have terminated (i.e. I_z switches from 0 to 1) when NSTOP consecutive positive peaks of z(t) exceed a prescribed threshold value z_T. Figure 15(c) shows a plot of the indicator function I_z for the lull/swell periods for nominal parameter values of NSTART = 2, NSTOP = 2 and z_T = 5.04 ft. The threshold value of z_T was chosen as the mean value of the positive peak amplitude envelope of z(t). Over the 100 s segment of data shown in Figure 15, the interval (602.2 - 644.4)s is identified as a swell period. In other words, the ongoing lull from t = 555 s is terminated at t = 602.2 s when two consecutive positive peaks of z(t) (i.e. NSTOP = 2) have exceeded the threshold of z_T = 5.04 ft (see Figure 15(a,c)). Similarly, a lull is initiated at t = 644.4 s when two consecutive positive peaks of z(t) (i.e. NSTART = 2) have stayed under the threshold of z_T = 5.04 ft (see Figure 15(a,c)).

Note that NSTOP = 2 results in true swells (i.e. swells which usually last for > 3 - 4 cycles or approximately $\geq$ 20 seconds) being detected one cycle after their actual onset. Selecting NSTOP = 1 would apparently solve this problem by detecting true swells one cycle earlier than with NSTOP = 2. However, this would create too many additional swells of 6 - 10 seconds duration due to the occurrence of isolated single peaks of z(t) exceeding the prescribed threshold z_T. The termination of lulls can be made one cycle earlier, when the first peak of z(t) exceeds z_T, if at that time one can confidently forecast that the next successive positive peak shall also exceed the prescribed threshold. This is illustrated in Figure 15(a,c), where the one cycle ahead forecasting based lull

termination occurs 5.4 seconds earlier at t = 596.8 s. Unfortunately, a reliable on-line one cycle ahead forecasting method is needed for practical implementation of the approach.

An alternative method for early detection of the onset of a swell based upon the z versus $\dot{z}$ phase plane pattern characteristics at lull/swell transitions was developed during this study. Phase plane plots of z(t) versus $\dot{z}(t)$ for several lull/swell transition segments (as defined by NSTOP = 2 and z_T = 5.04 ft) were analyzed to determine if a pattern or a sequence of events in the z and $\dot{z}$ time histories could be identified and used as a precursor for lull termination prior to the crossing of the threshold z_T by the second positive peak of z(t). Based on this analysis, a phase plane based criterion for lull termination that performs nearly as well as the one peak ahead forecasting based method was developed. According to this criterion, a lull is terminated if successive peak magnitudes of vertical position z(t) and vertical velocity $\dot{z}(t)$ (or $\dot{z}$ followed by z) exceed their prescribed thresholds. Thus, $I_{z,\dot{z}}$, the indicator function for this phase plane approach switches from zero to one according to Eq. (28).

$$I_{z,\dot{z}} \triangleq 1 \;:\; |z_{Peak}(t)| > z_T \text{ and } |\dot{z}_{Peak}(t^+)| > \dot{z}_T$$

$$\text{or} \qquad (28)$$

$$|\dot{z}_{Peak}(t)| > \dot{z}_T \text{ and } |z_{Peak}(t^+)| > z_T$$

where $\dot{z}_{Peak}(t^+)$ ($z_{Peak}(t^+)$) is the first peak in $\dot{z}(t)$ (z(t)) following the event $|z_{Peak}(t)| > z_T$ ($|\dot{z}_{Peak}(t)| > \dot{z}_T$). Figure 15(d) shows a plot of the resulting indicator function $I_{z,\dot{z}}$. Notice that the end of the lull is detected at t = 596.4 s. This compares favorably to the performance of the one peak ahead forecast based threshold test shown in Figure 15(c). This is further apparent on comparison of the indicator functions I_z and $I_{z,\dot{z}}$ over a period of 1200 seconds as shown in Figure 16.

The effects of varying NSTART (1,2 or 3) on $I_{z,\dot{z}}$ and hence lull/swell classification are shown in Figure 15 (e,d,f), respectively.

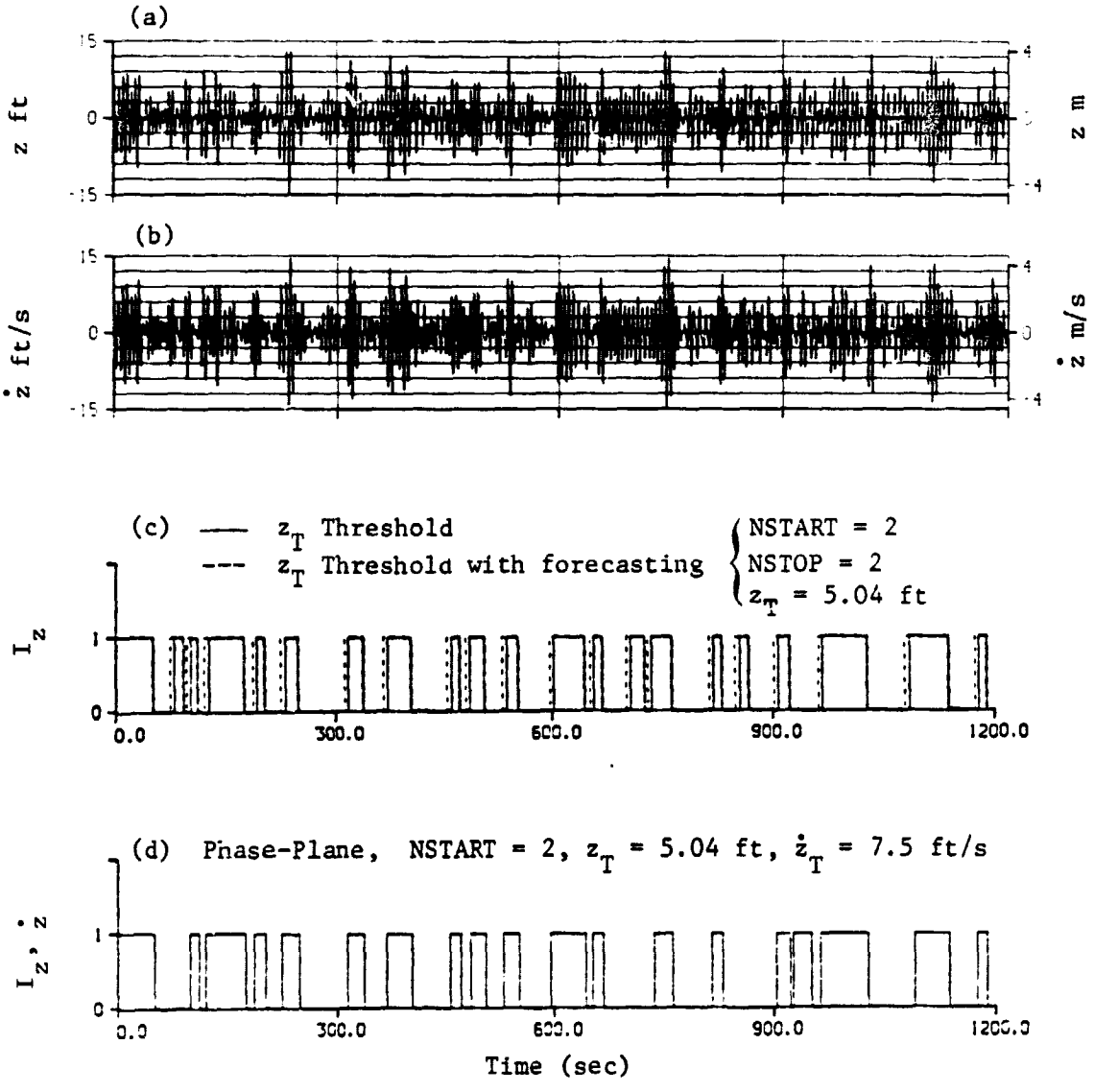

Figure 16. Comparison of I_z and I_z, $\dot{z}$ over a 1200 Second Period.

As expected, increasing NSTART values have an impact on lull/swell duration statistics. Figure 17 shows the survivor functions $\mathcal{F}(TL)$ and $\mathcal{F}(TI)$ for the lull duration and inter-lull (swell) interval, respectively, for NSTART = 1, 2 and 3. These plots show that the principal effect of increasing NSTART is on the swell interval statistics, and most significantly on the likelihood of swell periods of two minutes and longer. A go/no go guidance command based upon a lull/swell classification algorithm with such parameters (NSTART = 3) could result in a no-go command lasting for two minutes or longer, which would be unacceptable because of constraints imposed by pilot workload, fuel reserves, and other operational considerations. Therefore, either NSTART = 1 or 2 may be used to define the initiation of a lull. A value of NSTART = 2 was selected as nominal during this study.

Figure 18 shows the histograms of $\dot{z}$, $\dot{y}$, $\ddot{y}$ and $\dot{\phi}$ during lull and swell periods corresponding to the $I_{z,\dot{z}}$ phase plane indicator function shown in Figure 16(d). These histograms show that the standard deviations of the variables $\dot{z}$, $\dot{y}$, $\ddot{y}$ and $\dot{\phi}$ have significantly lower values during lull periods in comparison to their values during swell intervals. Therefore, improvements in the touchdown performance should be possible if shipboard landings can be restricted to occur during lull periods alone.

The lull and swell duration survival functions $\mathcal{F}(TL)$ and $\mathcal{F}(TI)$ for the three options of lull termination shown in Figure 15(c,d), namely a) z threshold, b) z threshold with one peak ahead forecasting, and c) $z,\dot{z}$ phase plane, are plotted in Figure 19. The plots show that the options (b) and (c) above are nearly the same. However, they give slight lower (higher) values of the lull (swell) duration survival functions than option (a).

In summary, a generic structure for an on-line/swell classification algorithm has been developed. The selection of the threshold values z_T and $\dot{z}_T$, and parameter NSTART define the lull/swell classification rule and the resulting temporal and statistical characteristics of the lull and swell patterns.

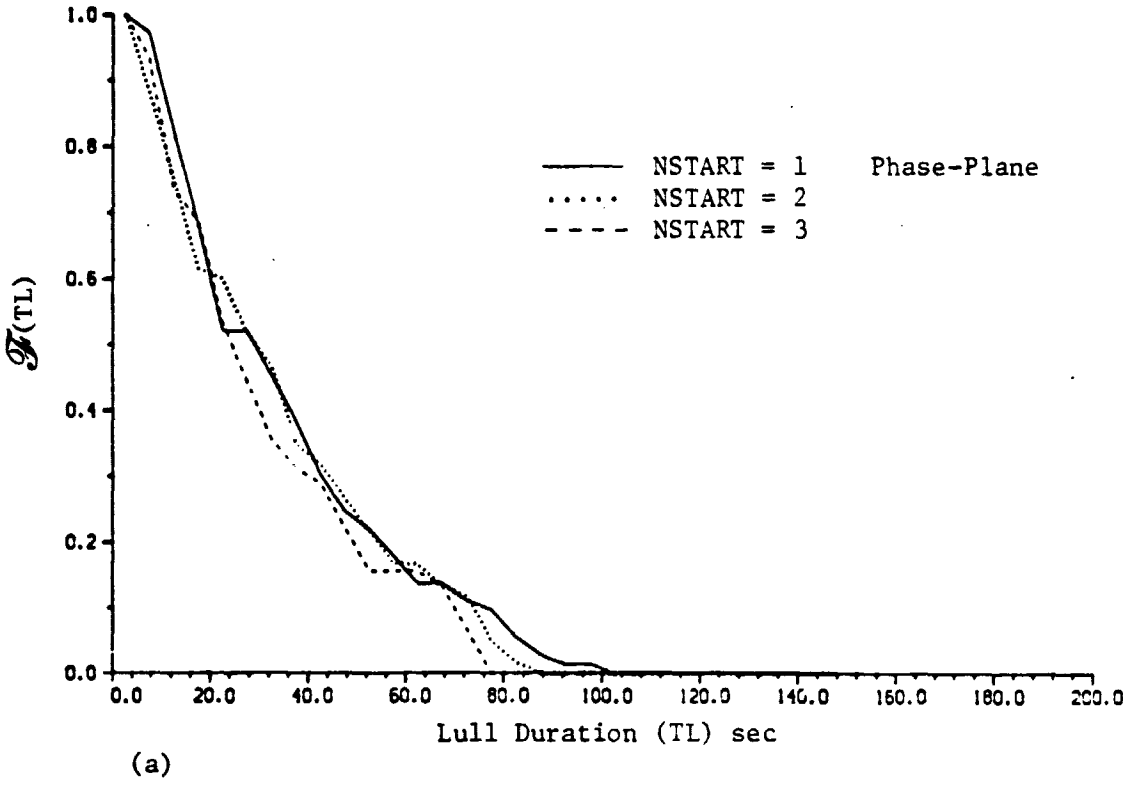

(a)

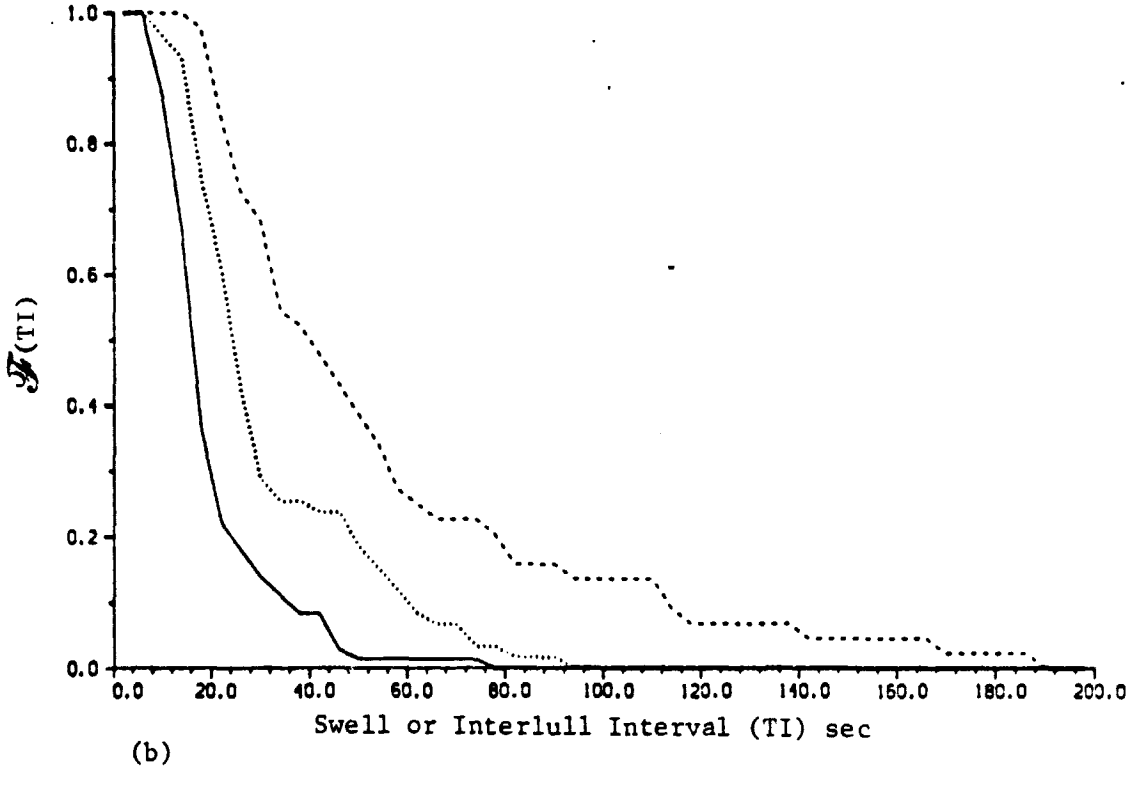

(b)

Figure 17. Survivor Functions $\mathscr{F}$(TL) and $\mathscr{F}$(TI) for Lull Duration TL and Swell Interval TI.

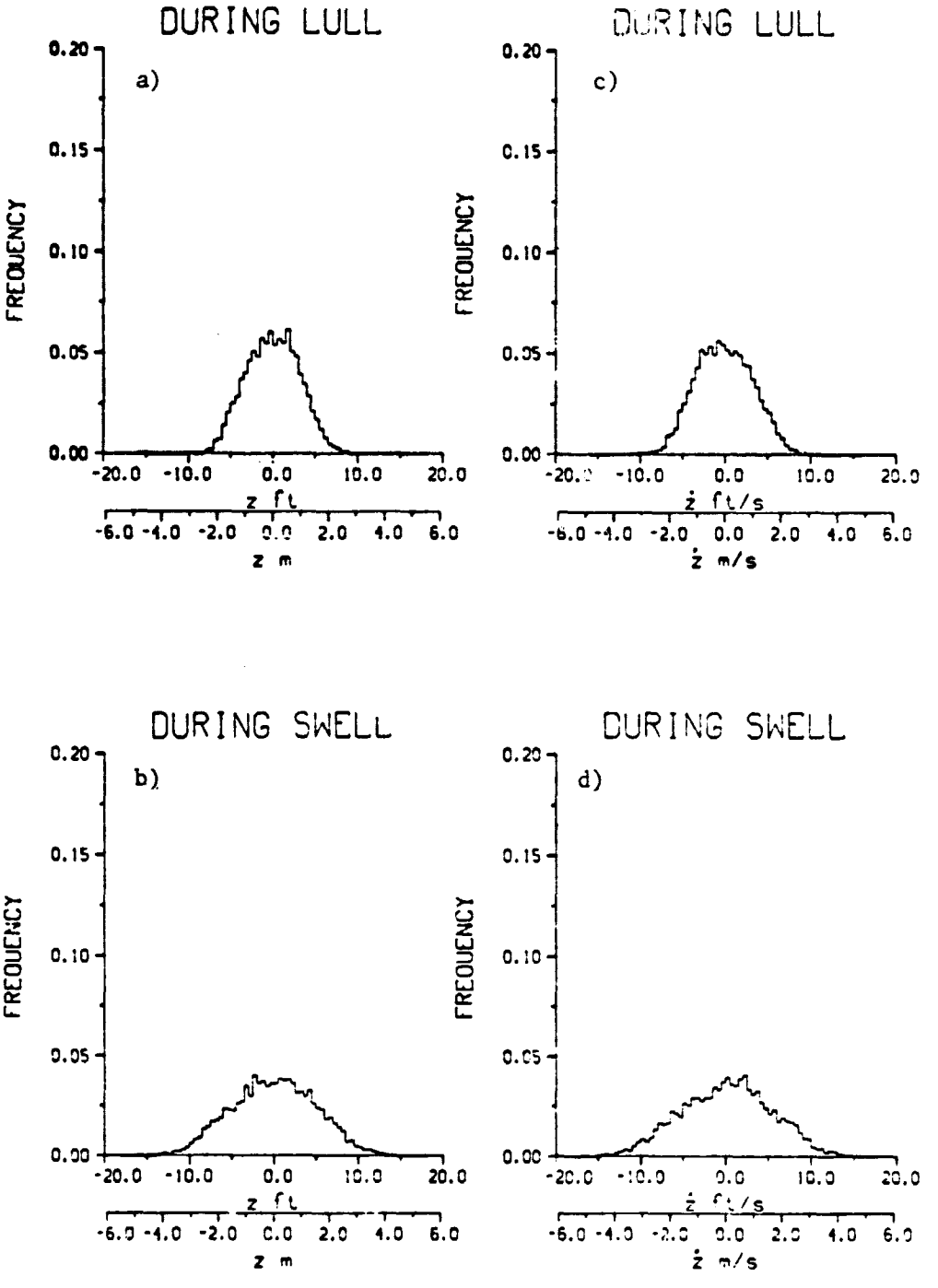

Figure 18. Lull/Swell Amplitude Histograms for z and $\dot{z}$ with $I_{z,\dot{z}}$ and z_T = 5.04 ft, $\dot{z}_T$ = 7.5 ft/s, NSTART = 2.

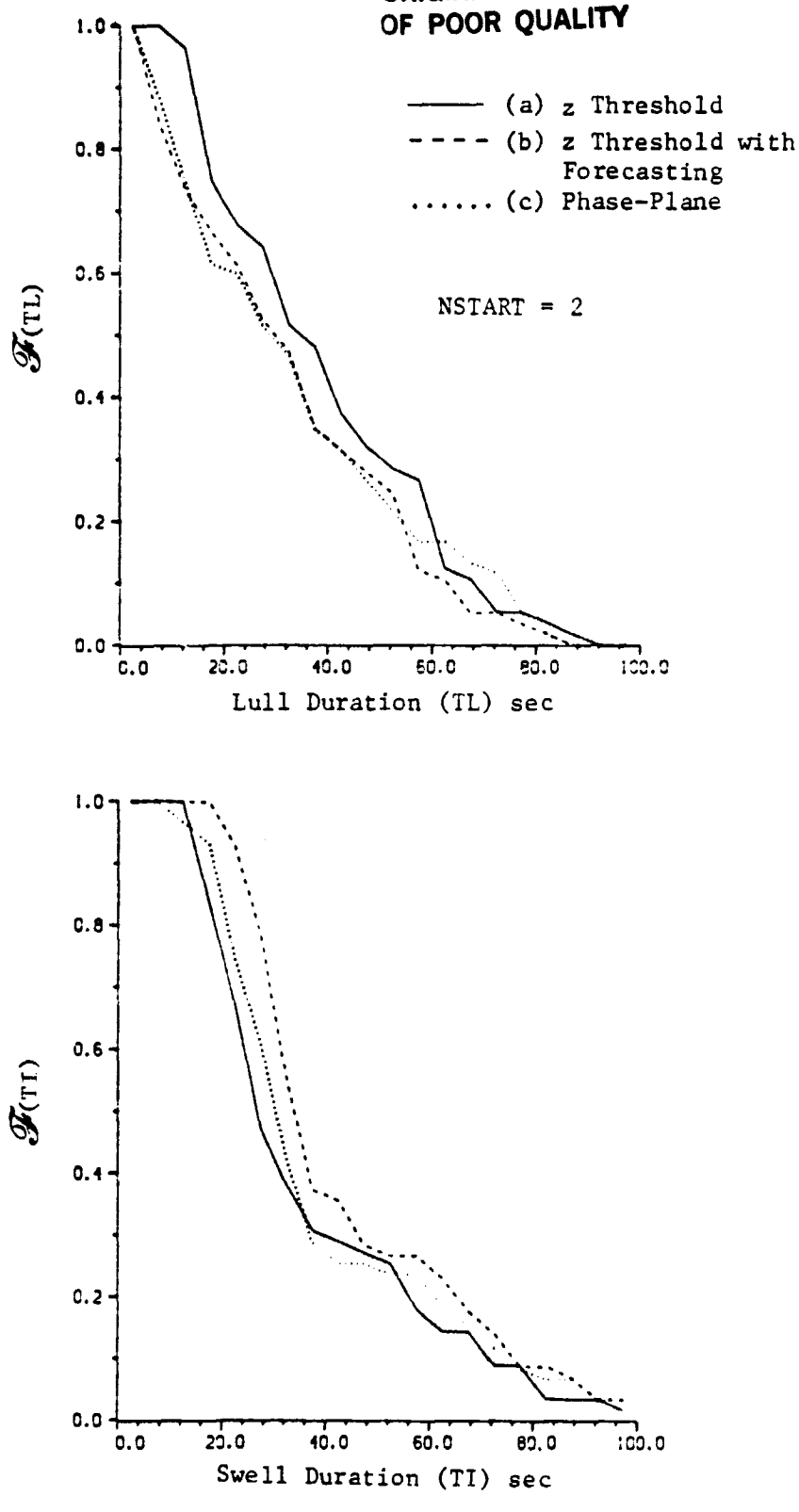

Figure 19. Lull and Swell Duration Histograms for Three Lull Termination Options.

The next section is devoted to an evaluation of alternative pattern based letdown guidance schemes. Improvements in touchdown performance obtained using a lull directed adaptive letdown guidance strategy are presented.

4. SHIP MOTION PATTERN DIRECTED LETDOWN GUIDANCE

The purpose of this section is to investigate the potential improvement in touchdown performance that can be achieved with a lull/swell pattern directed letdown guidance strategy. Three different lull/swell classification schemes described in the previous section are considered. They are:

Scheme (a) lull/swell classification based upon the use of a heave amplitude threshold (z_T) driven indicator function I_z with z_T = 5.04 ft, NSTART = 2 and NSTOP = 2 (see Fig. 16, dark switch plot in I_z);

Scheme (b) lull/swell classification based upon the use of indicator function I_z as in (a) above but with the additional capability of one peak ahead forecasting or prediction (see Fig. 16, dotted switch plot in I_z); and

Scheme (c) lull/swell classification based upon the use of a deck vertical motion phase plane threshold (z_T, $\dot{z}_T$) driven indicator function - $I_{z,\dot{z}}$ with z_T = 5.04 ft, $\dot{z}_T$ = 7.5 ft/s, and NSTART = 2.

A CROD (-2 ft/s) letdown profile may be initiated at any time during a lull period. Three options are available at the termination of a lull with respect to the future trajectory of ongoing letdown profiles, as follows:

Option (1): Continue ongoing CROD letdown profile until termination at touchdown.

Option (2): Arrest the aircraft rate-of-descent and hold the altitude of the aircraft at lull termination until touchdown.

Option (3): Abort the aircraft rate-of-descent, initiate maximum rate-of-climb, and return to the prescribed hover altitude.

Eight alternative letdown guidance strategies defined in Table 2 were simulated and analyzed. Strategy #0 represents the nominal CROD letdown guidance profile discussed earlier in Section 2.3. An off line computer simulation of the landing task was conducted to generate the touchdown performance statistics. Letdown profiles from the hover point until touchdown were initiated every one (1) second when permitted to do so by the particular guidance strategy. Touchdown performance is presented in terms of the survival functions for $\dot{z}_R$, $|\dot{\phi}|$ and $|\dot{y}|$. The results are presented in two formats - plots and tables. Figure 20 shows the survival function $\mathscr{F}(\dot{z}_R)$ for letdown guidance strategies 0 through 3, respectively. Similarly, Figure 21 shows $\mathscr{F}(\dot{z}_R)$ for letdown guidance strategies #0, #4, #5, #6, and #7. Survival functions for $\dot{z}_R$, $|\dot{y}|$ and $|\dot{\phi}|$ are tabulated in Tables 3-5, respectively.

Figure 20 shows that there is no significant difference in the survival functions $\mathscr{F}(\dot{z}_R)$ for the four strategies 0 thru 3. In other words, no improvement is obtained by using a letdown guidance strategy wherein the decision to initiate a letdown ("go" decision) is restricted to lull periods alone. This is because the problem lies at the termination of a lull with the letdown profiles already initiated in the past ten (10) seconds and which have not yet landed. The result is that these profiles terminate in touchdowns during swell ("no go" decision) intervals, when deck vertical velocity $\dot{z}$ can be high. Thus, for guidance strategies 1 through 3, although the actual number of touchdowns with large relative impact velocities (e.g., $\dot{z}_R > 12$ ft/s) is lower, the percentage of these touchdowns with respect to the total number of touchdowns is not significantly different from that for the nominal CROD letdown strategy #0.

Letdown profile options (2) and (3) provide a way for handling these ongoing landings at the instant of lull to swell transition. In option (2), the number of touchdowns during a swell interval, as well as the relative vertical impact velocities at touchdown, is reduced by switching the letdown rate-of-descent from -2 ft/s to zero at lull termination. Thereafter, the aircraft is maintained in an altitude hold mode until touchdown during a swell or until the initiation of the next lull period ("go" decision) when

TABLE 2

Alternative Letdown Guidance Strategies

Letdown Guidance Strategy #	Lull/Swell Classification Scheme	Letdown Profile Option at Lull Termination
0	None	N/A CROD Letdown
1	(a)	(1)
2	(b)	(1)
3	(c)	(1)
4	(a)	(2)
5	(b)	(2)
6	(c)	(2)
7	(c)	(3)

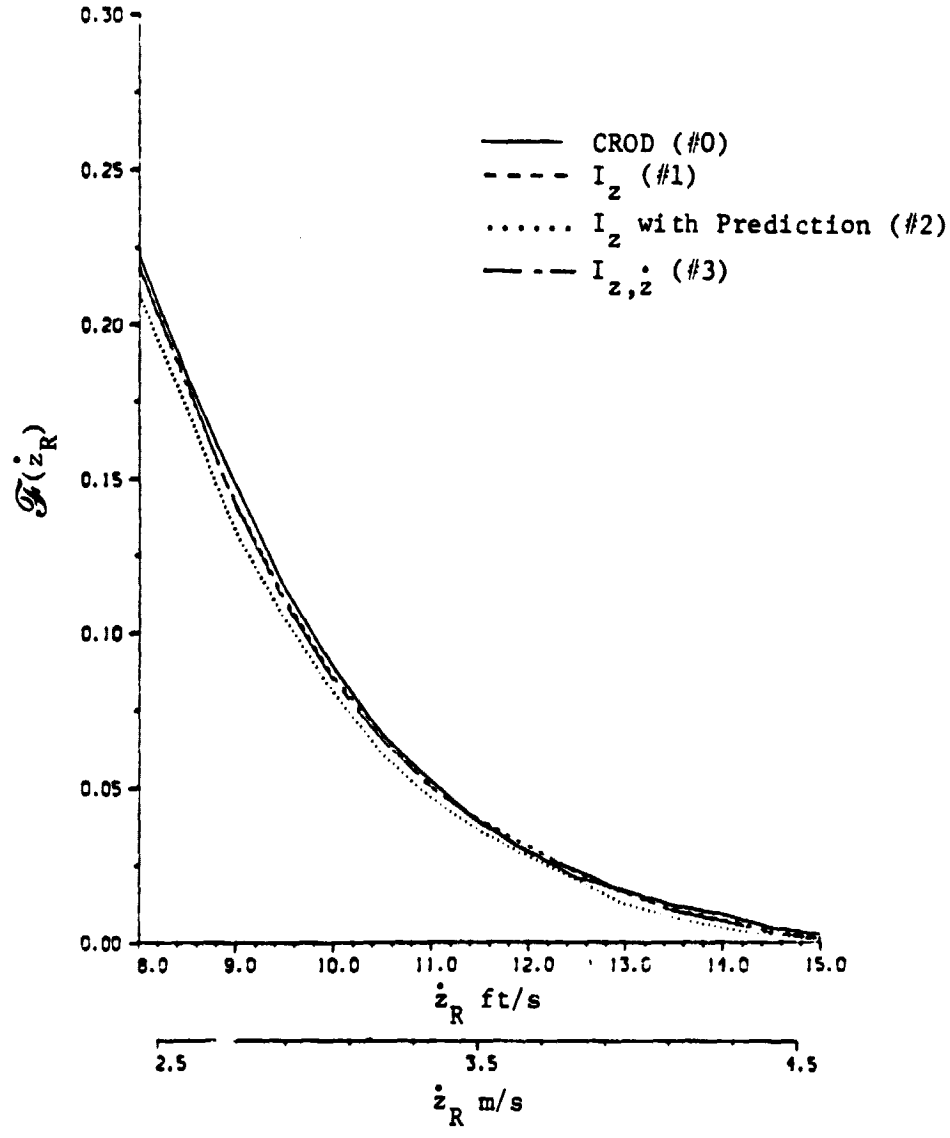

Figure 20. $\mathscr{F}(\dot{z}_R)$ at Touchdown for Alternative Lull Classification Schemes and CROD Letdown.

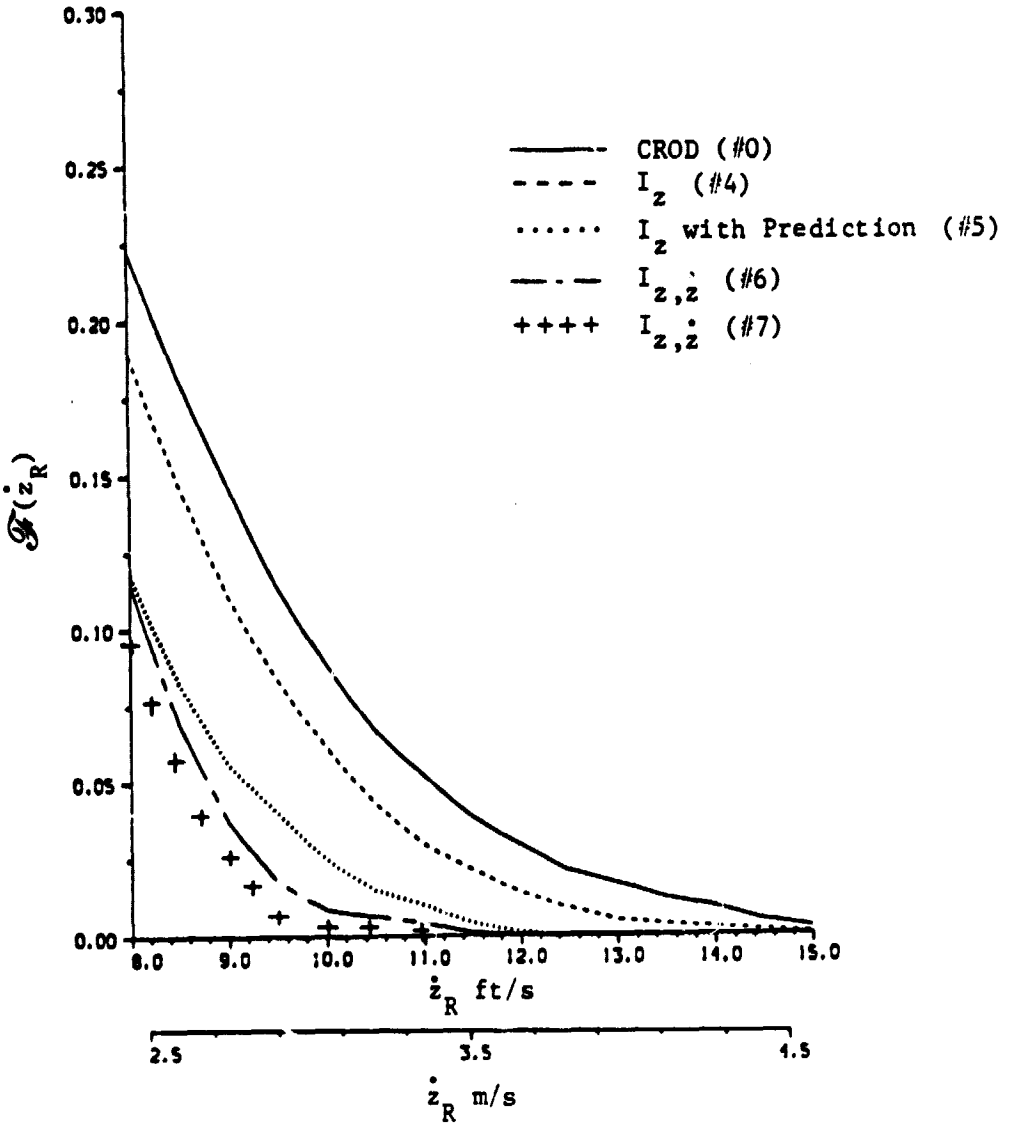

Figure 21. Comparison of $\mathscr{F}(\dot{z}_R)$ for Alternative Lull Pattern Directed CROD Letdown Guidance Scheme.

TABLE 3

$\lvert\dot{y}\rvert$ ft/s	$\mathcal{F}(\lvert\dot{y}\rvert)$ x 100% Letdown Guidance Strategy #							
	0	1	2	3	4	5	6	7
2	54	52	50	52	52	48	51	43
4	19	18	16	17	17	14	16	11
5	9	9	7	9	9	7	8	4
7	2	1	1	1	1	1	1	0

TABLE 4

$\lvert\dot{\phi}\rvert$ deg/s	$\mathcal{F}(\lvert\dot{\phi}\rvert)$ x 100% Letdown Guidance Strategy #							
	0	1	2	3	4	5	6	7
2	44	43	41	43	43	38	41	33
3	23	22	21	22	22	18	20	14
4	10	10	8	9	9.5	7	8	5
5	3	3	2	3	3	2	3	1

TABLE 5

$\dot{z}_R$	$\mathcal{F}(\dot{z}_R)$ x 100%							
	Letdown Guidance Strategy #							
ft/s	0	1	2	3	4	5	6	7
8	22	22	21	22	19	12	11	10
10	9	9	8	9	6	2.5	1	0
12	3	3	3	3	1	0	0	0

the CROD letdown profile is resumed to touchdown. In option (3), any ongoing CROD profiles are aborted at the instant of lull termination. Survival functions $\mathcal{F}(\dot{z}_R)$ for letdown guidance strategies #0, #4, #5, #6, and #7 are shown in Figure 21. These plots show that touchdown vertical velocities are lowest for option #7 and monotonically increase for option #6, #5, #4 and 0, in that order.

Survival functions for $|\dot{y}|$ and $|\dot{\phi}|$ at touchdown are given in Tables 3 and 4 respectively. Table 5 presents the results of Figures 20-21 for $\mathcal{F}(\dot{z}_R)$ in a tabular format. Results for $\mathcal{F}(|\ddot{y}|)$ are not included because there were not any noticeable differences in touchdown performance across the eight letdown guidance strategies. A review of these data indicates that the most significant improvements in touchdown performance occur for letdown guidance strategy #7. For example, strategy #7 decreases the probability of exceeding touchdown vertical impact velocities of 10 ft/s from 9% for the CROD letdown strategy (#0) to ≈0%, an order of magnitude improvement. Similar improvements are obtained in touchdown values for relative lateral impact velocity $|\dot{y}|$ and relative roll rate $|\dot{\phi}|$.

In summary, the results clearly demonstrate the inherent potential of a go/no-go letdown guidance strategy which only allows letdown profiles that begin and terminate during lull periods. Fine tuning of such a guidance methodology would be necessary with the actual shipboard landing scenario under consideration.

5. CONCLUSIONS AND RECOMMENDATIONS

A computer simulation of the VTOL shipboard landing task was developed and used to investigate alternative letdown guidance system concepts. The NAVAIRENGCEN Ship Motion Computer Program [1] was used to generate simulated ship/deck motion time history data for a Spruance class destroyer (DD963) operating in rough seas (sea state > 5), at a speed (V_s) of 25 kts with a heading (μ_s) of 120°. The program uses a sum of sinusoids approximation to the ship motion spectra in each of the six degrees of freedom for generating the time response data.

Touchdown performance was evaluated in terms of the survival functions (i.e., Probability of variable X exceeding a level x or Pr [X > x]) for four key variables - vertical impact velocity $\dot{z}_R (\equiv \dot{z}_P - \dot{z}_A)$, magnitudes of lateral impact velocity ($|\dot{y}|$) and acceleration ($|\ddot{y}|$), and magnitude of relative roll rate $|\dot{\phi}|$. The touchdown performance of a constant rate-of-descent (CROD) letdown scheme was used as a baseline against which the performance of alternative letdown guidance systems was compared.

Two categories of alternative letdown guidance concepts were considered: (1) designs that exploit the existence of quiescent ship motion called lulls, and (2) designs that do not depend upon a lull/swell pattern in ship motion. The latter approach requires the development of letdown control laws based upon ship motion following and/or forecasting schemes. However, actual ship motion time histories exhibit a clearly recognizable pattern of alternating lulls and swells, which may be used for improving touchdown performance. Therefore, this study was restricted to the investigation of alternative ship motion pattern directed letdown guidance algorithms. A real time algorithm for lull/swell classification based upon ship motion pattern features (e.g., phase-plane method) was developed. The classification algorithm was used to command a go/no go signal to direct the initiation/termination of an acceptable landing window.

The temporal characteristics of the simulated ship motion time histories were shown to be intimately dependent upon the number of sinusoids (N) used to represent the motion spectra. In particular, the lull/swell pattern of ship motion becomes increasingly evident with the growth in the number of sinusoidal components. The results show that a sum of six sinusoids [as suggested in reference 5] representation does not display a pattern of alternating lull/swell intervals. Therefore, a sum of seventy sinusoids was selected as being adequate for describing the known ship motion characteristics.

Results of the shipboard landing simulation show that substantial improvements over CROD touchdown performance may be achieved by using a lull/swell pattern directed letdown guidance where touchdowns are permitted only during lull periods. For example, the probability of exceeding touchdown vertical impact velocities of 10 ft/s is reduced from 9% for the CROD strategy to 0% for the lull/swell pattern directed guidance strategy - an order of magnitude improvement. Similar improvements are obtained across a wide range of values for variables $\dot{z}_R$, $|\dot{y}|$ and $|\dot{\phi}|$.

Based upon the results of this study, the following plan for further research is recommended:

1. Analysis of Actual Ship Motion Data.

The purpose of this task would be to assess the validity of the ship motion pattern analysis results obtained from the sum of sinusoids model with actual data. Any discrepancies between simulated and actual data must be analyzed to determine their impact upon the lull/swell pattern statistics and the touchdown performance obtained with the pattern based letdown guidance strategy.

2. Piloted Simulation Experiments.

The objective of these experiments would be to evaluate the potential usefulness of alternative ship motion pattern based letdown guidance schemes on manual shipboard landing performance. Four letdown guidance options are proposed:

a. Letdown with no guidance

b. Letdown with a go/no go guidance (e.g., ship mounted or heads up green/red signal)

c. Letdown with roll/heave stabilized horizon bar display (ship mounted or heads up display)

d. Letdown with a go/no go guidance and roll/heave stabilized horizon display (i.e., options b and c).

The purpose of the option (c) would be to determine if the pilot is capable of learning the lull/swell pattern from observing the ship motion with respect to the roll/heave stabilized horizon bar.

3. Analysis of Data from Piloted Simulation Experiments.

The objective of this task would be to analyze the data gathered from the piloted simulation experiments with a view towards determining the relative merits of the four alternative letdown guidance laws. An understanding of this data would be used to develop an improved letdown guidance scheme.

REFERENCES

1. Brown, R.G., and Camaratta, F.A., NAVAIRENGCEN Ship Motion Computer Program, NAEC Report NAEC MISC-903-8, 1978.

2. St. Denis, M., and Pierson, W.J., On the Motions of Ships in Confused Seas, Transactions of the Society of Naval Architects and Marine Engineers, Vol. 61, pp 280-357, 1953.

3. Meyers, W.G., Sheridan, D.J., and Salveson, N., NSRDC Ship Motion and Sea Load Computer Program, NSRDC Report 3376, February 1975.

4. Baitis, A.E. and Wollaver, D.A., Trial Results on Ship Motions and Their Influence on Aircraft Operations for ISCS Guam, NSRDC Report 525-H-01, February 1974.

5. Fortenbaugh, R.L., Progress in Mathematical Modeling of the Aircraft Operational Environment of DD963 Class Ships, AIAA Atmospheric Flight Mechanics Conference, Boulder, CO, August 1979.

6. McGee, L.A., Paulk, C.H., Steck, S.A., Schmidt, S.F., and Merz, A.W., Evaluation of the Navigation Performance of Shipboard - VTOL - Landing Guidance Systems, AIAA Guidance and Control Conference, Boulder, CO, August 1979.

7. Sorensen, J.A., Goka, T., Phatak, A.V., and Schmidt, S.F., An Investigation of Automatic Guidance Concepts to Steer a VTOL Aircraft to a Small Aviation Ship, NASA CR-152407, July 1980.

8. McMuldroch, C.G., Stein, G. and Athans, M., VTOL Control for Shipboard Landing in High Sea States, 18th IEEE Conf. on Decision and Control, December 1979.

9. Box, G.E.P. and Jenkins, G.M. (1970), Time Series Analysis: Forecasting and Control. San Francisco, Holden-Day.